

CHAPTER 2

Zeolite Structures

STEF SMEETS AND XIAODONG ZOU*

Berzelli Centre EXSELENT on Porous Materials, Department of Materials and Environmental Chemistry, Stockholm University, SE-106 91 Stockholm, Sweden

*Email: xzou@mmk.su.se

2.1 Introduction

A zeolite is an open framework material consisting of a three-dimensional, four-connected network of corner-sharing TO_4 tetrahedra, where the T-atoms are tetrahedrally connected atoms bridged by O-atoms. Understanding the regular (and sometimes irregular) arrangement of the atoms in a zeolite structure is key to understanding why and how the zeolite functions, and to improving its properties and performance. A zeolite's performance is essentially determined by its structural characteristics, such as the dimensionality of its channels, the accessible pore volume, the size of the pore openings, and the number and placement of extra-framework species. A zeolite is defined by its framework structure.

Traditionally, zeolites are aluminosilicate framework materials, but now high- or pure-silica (SiO_2) zeolites can also be produced, and the Si can be substituted by heteroatoms such as Ge, B, Al, Ga, Zn, Be, P, *etc.* The placement of heteroatoms in the zeolite framework structure influences its function. For example, Al has fewer electrons in the outer shell than does Si, so it introduces a local negative charge into the framework that is compensated by exchangeable extra-framework cations. An extensive array of cations with different catalytic properties can be introduced into the zeolite

RSC Catalysis Series No. 28

Zeolites in Catalysis: Properties and Applications

Edited by Jiří Čejka, Russell E. Morris and Petr Nachtigall

© The Royal Society of Chemistry 2017

Published by the Royal Society of Chemistry, www.rsc.org

at such sites, and this can have profound consequences on any reaction that is acid- or metal-catalysed. 1

Zeolites are a class of microporous materials, with cavities and channel systems of molecular dimensions (typically $<20 \text{ \AA}$), and this makes them useful as molecular sieves. It is the combination of this feature with a zeolite's catalytic properties that makes it a shape-selective catalyst, exploiting both properties to control the selectivity of catalytic reactions. As a result, zeolites have found widespread applications as catalysts, adsorbents, molecular sieves, and ion-exchangers and are among the most important catalysts in the oil refining, petrochemical, and fine chemical industries. 5 10

A zeolite's framework structure therefore dictates its function. Normally, several analytical techniques are combined to probe the fine structural details of a material. Sorption experiments can be used to probe pore size and accessibility. Diffraction techniques are used to determine the average framework structure, including the location of heteroatoms, extra-framework species, and cations. Solid-state NMR will give information about the local structure, such as the connectivity of Si, or the preferential location of Ge at specific sites. Electron microscopy can be used to directly visualize a zeolite's channel system along a particular direction and characterize stacking faults. 15 20

The following sections of this chapter will cover (1) how zeolites are described by their framework type, (2) a discussion of the 'decoration' of the framework, and how this influences the structure, (3) some real-world examples of how structure and chemistry are closely related, and (4) a brief overview of structure determination by powder diffraction and electron crystallography. 25

2.2 Zeolite Framework Types

2.2.1 Classification 30

Because of the importance of zeolites in various industrial applications, many laboratories have tried to produce new zeolites. The number of new materials discovered boomed in the 1970s. It became clear that different laboratories were producing similar materials, with the same framework type, but under different names, and perhaps under different synthesis conditions, and with different chemical compositions. In an attempt to bring some order into this chaos and to categorize the zeolites, Meier and Olson proposed the use of framework types to classify zeolite materials. They produced the first edition of *Atlas of Zeolite Structure Types* – a compilation of all the known framework types,¹ each of which was assigned a three-letter code derived from the name of the zeolite or 'type material'. For example, zeolites X and Y have the same framework topology as the natural mineral *faujasite*, and are therefore assigned the code **FAU**, Linde Type A served as the type material for the code **LTA**, and ZSM-five for **MFI**. The original print of the Atlas, featuring **MFI** on the front cover (the most complicated zeolite 35 40 45

known at the time), contained 38 codes, including wire-frame stereo drawings of the frameworks and a description of their crystal structures, symmetries, and type materials. Notice the subtle difference here between a framework *structure* and framework *type*. A framework type (sometimes referred to as topology) simply describes the connectivity of the T-atoms in the highest possible symmetry, and does not depend on composition, distribution of the T-atoms, guest species in the pores, symmetry, or cell dimensions. Nowadays, the codes are assigned by the Structure Commission of the International Zeolite Association, which is officially recognized by IUPAC. Framework type codes (FTCs) are capitalized and written using a bold typeface. A minus (–) sign is used to indicate interrupted frameworks (e.g. –**ITV** or –**SVR**), and an asterisk (*) for disordered frameworks (e.g. ***BEA** or ***SFV**), but a combination is also possible (e.g. *–**SSO** or *–**EWT**). Materials can be described using the IUPAC crystal chemical formula, where guest species are enclosed in vertical bars ($|\cdot\cdot\cdot|$) and the framework host in square brackets ($[\cdot\cdot\cdot]$). For example, the aluminophosphate version of **CHA** (*chabazite*) can be designated as $[\text{Al-P-O}]\text{-CHA}$ to distinguish it from the aluminosilicate type material: $[\text{Al-Si-O}]\text{-CHA}$. The full notation for the latter would be $|\text{Ca}_6(\text{H}_2\text{O})_{40}|[\text{Al}_{12}\text{Si}_{24}\text{O}_{72}]\text{-CHA}$.

2.2.2 Database of Zeolite Structures

The most up-to-date database of framework types can only be found online at <http://www.iza-structure.org/databases/>, and contained 232 different framework codes as of October 2016. Newly approved framework types are announced on the IZA Structure commission's website (<http://www.iza-structure.org/>). The starting page of the Database of Zeolite Structures shown in Figure 2.1 provides an overview of all the framework type codes assigned to date. By clicking on any of the three-letter codes, the user navigates to a page containing detailed information about the framework corresponding to the selected code. An example for **FAU** is shown in Figure 2.2. This page contains information on the idealized framework (highest symmetry, geometry optimized for SiO_2), the unit cell and space group symmetry, framework and topological density, ring sizes and channel system, size of the cavity and free diameters of the windows, accessible volume, the building units and natural tilings that can be used to describe the framework, a crystallographic information file (CIF) with the coordinates of the framework atoms, and a list of coordination sequences and vertex symbols. Most of these concepts are described in more detail below. From this page, the user can also look up information on the Type Material and Related Materials (with references to known zeolites with the same framework type), view a 3D model of the framework type, or generate a powder diffraction pattern. As an example the Type Material page of **FAU** is shown in Figure 2.3. Lastly, the database also contains an advanced search function to select frameworks with any of the physical properties mentioned here.

Database of Zeolite Structures

Zeolite Framework Types

Search for a Framework Type Code (FTC)

(Two or more letters/numbers; also search for a material that contains this string)

or select an FTC from the table:

ABW	ACO	AEI	AEL	AEN	AET	AFG	AFI	AFN	AFO	AFR	AFS
AFT	AFV	AFX	AFY	AHT	ANA	APC	APD	AST	ASV	ATN	ATO
ATS	ATT	ATV	AVL	AWO	AWW	BCT	*BEA	BEC	BIK	BOF	BOG
BOZ	BPH	BRE	BSV	CAN	CAS	CDO	CFI	CGF	CGS	CHA	-CHI
-CLO	CON	CSV	CZP	DAC	DDR	DFO	DFT	DOH	DON	EAB	EDI
EEL	EMT	EON	EPI	ERI	ESV	ETL	ETR	EUO	*-EWT	EZT	FAR
FAU	FER	FRA	GIS	GIU	GME	GON	GOO	HEU	IFO	IFR	-IFU
IFW	IFY	IHW	IMF	IRN	IRR	-JRY	ISV	ITE	ITG	ITH	*-ITN
ITR	ITT	-ITV	ITW	IWR	IWS	IWV	IWW	JBW	JNT	JOZ	JRY
JSN	JSR	JST	JSW	KFI	LAU	LEV	LIO	-LIT	LOS	LOV	LTJ
LTF	LTJ	LTL	LTN	MAR	MAZ	MEI	MEL	MEP	MER	MFI	MFS
MON	MOR	MOZ	*MRE	MSE	MSO	MTF	MTN	MTT	MTW	MVY	MWF
MWW	NAB	NAT	NES	NON	NPO	NPT	NSI	OBW	OFF	OKO	OSI
OSO	OWE	-PAR	PAU	PCR	PHI	PON	POS	PSI	PUN	RHO	-RON
RRO	RSN	RTE	RTH	RUT	RWR	RWY	SAF	SAO	SAS	SAT	SAV
SBE	SBN	SBS	SBT	SEW	SFE	SFF	SFG	SFH	SFN	SFO	SFS
*SFV	SFW	SGT	SIV	SOD	SOF	SOS	SSF	*-SSO	SSY	STF	STI
*STO	STT	STW	-SVR	SVV	SZR	TER	THO	TOL	TON	TSC	TUN
UEI	UFI	UOS	UOV	UOZ	USI	UTL	UWY	VET	VFI	VNI	VSV
WEI	-WEN	YUG	ZON								

Figure 2.1 Overview of the 232 zeolite framework type codes accessible *via* the online zeolite structure database, with permission from the Database of Zeolite Structures.

2.2.3 Channels

Zeolite structures are almost always described first in terms of pore size and dimensionality. Each channel is classified by the number of T-atoms delimiting the smallest pore opening. Channels delimited by an 8-ring are considered small (free diameter of ~ 4.0 Å), 10-rings medium (~ 5.5 Å), 12-rings large (~ 7.0 Å), and anything above that is extra-large. The free diameters of the type materials are given as an indication of the pore size, and calculated using an oxygen van der Waals radius of 1.35 Å. Note that rings may be somewhat distorted, depending on the symmetry and the surroundings of the delimiting T-atoms, and this affects the pore dimensions. Therefore, the pore size is usually given by its minimum and maximum dimensions. The channel systems can be multidimensional, and are of molecular dimensions. Therefore, zeolites normally have at least one 8-ring or larger channel.

Database of Zeolite Structures

Framework Type FAU

Framework ⓘ

Space Group: Fd-3m (origin choice 2) (# 230)

Cell Parameters:

a = 24.345 Å	b = 24.345 Å	c = 24.345 Å
$\alpha = 90.000^\circ$	$\beta = 90.000^\circ$	$\gamma = 90.000^\circ$
Volume =	14428.77Å ³	
R _{0LS} =	0.0009	

Framework density (FD_S): ⓘ 13.3 T/1000 Å³

Topological density: ⓘ TD₁₀ = 579 TD = 0.476190

Ring sizes (# T-atoms): 12 6 4

Channel system: 3-dimensional

Maximum diameter of a sphere: ⓘ


that can be included 11.24Å

that can diffuse along a: 7.35Å b: 7.35Å c: 7.35Å


Accessible volume: 27.4 % (additional data)

Secondary Building Units: ⓘ 6-6 or 6-2 or 6 or 4-2 or 1-4-1 (List of all SBUs) or 4

Composite Building Units: ⓘ (List of all CBUs)



d6r (t-hpr)



sod (t-toc)

Natural Tiling ⓘ (List of Tiles)

t-fau t-hpr t-toc

Tiling arrangement 3d Tilings display

Coordinates: List (T-atoms), CIF (T and O atoms)

Coordination sequences: ⓘ List

+ Vertex symbols ⓘ

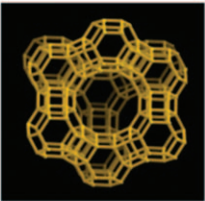
+ Loop configurations ⓘ

Year code assigned 1978

Data last updated (M/D/Y) Jul 1, 2007

Copyright © 2008 Structure Commission of the International Zeolite Association (IZA-SC)

Click on any of the images below to get a larger version



Viewed along [111]

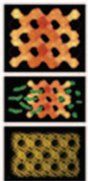


Figure 2.2 Landing page for framework type FAU, with permission from the Database of Zeolite Structures.

The channel systems are defined by the channel directions relative to the crystallographic axes.

2.2.4 Building Units

The common feature of all zeolites is that they are built up of corner-sharing TO₄ tetrahedra forming a three-dimensional, four-connected network. These tetrahedra are the primary or basic building units (BBUs) that can always be assembled to form the framework of a zeolite. However, to describe structural features of zeolites, and highlight commonalities, they are not very useful. Researchers have come up with several higher order schemes and groupings to break down a zeolite framework into units larger than BBUs.

Database of Zeolite Structures

Framework Type FAU

Type Material

Material Name: Faujasite
Chemical Formula: $[(Ca^{2+}, Mg^{2+}, Na^+)_{29} (H_2O)_{240}] [Al_{58}Si_{134} O_{384}] \cdot FAU$
Unit Cell:
 cubic Fd-3m (# 227)
 $a = 24.74 \text{ \AA}$ $b = 24.74 \text{ \AA}$ $c = 24.74 \text{ \AA}$
 $\alpha = 90^\circ$ $\beta = 90^\circ$ $\gamma = 90^\circ$
Framework density: 12.7 T/1000 \AA^3
Channels: $\langle 111 \rangle$ 12 7.4 x 7.4*** (3-dimensional)

12-ring viewed along $\langle 111 \rangle$

References:
 Baur, W.H. "On the cation and water positions in faujasite", *Am. Mineral.*, **49**, 697-704 (1964)
 Bergerhoff, G., Baur, W.H. and Nowacki, W. "Über die Kristallstrukturen des Faujasits", *N. Jb. Miner. Mh.*, 193-200 (1958)

Copyright © 2007 Structure Commission of the International Zeolite Association (IZA-SC)

Figure 2.3 Type material page for framework type FAU, with permission from the Database of Zeolite Structures.

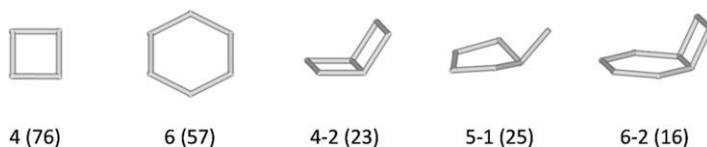


Figure 2.4 A selection of some of the most common SBUs. The number in parenthesis corresponds to the occurrence of the SBU.

The most common of these schemes, secondary building units (SBUs), composite building units (CBUs), and natural tiles (also known as natural building units; NBUs), are discussed below.

Secondary building units (SBUs) were initially derived with the idea that an entire framework could be built using a single SBU. SBUs are non-chiral units with up to 16 T-atoms. At present, the Database of Zeolite Structures contains 23 different SBUs, which can be found *via* framework type pages (Figure 2.2) by clicking on *List of all SBUs*. Some of the most frequently occurring SBUs are shown in Figure 2.4. Because of the increasing complexity of the new zeolites discovered during the past decade it became impossible to describe all framework structures in terms of a single SBU – often two or more are needed. For this reason, SBUs are no longer generated for the newer frameworks in the Database. Instead, composite building units (CBUs) are used to describe these structures.

CBUs merely represent common structural features present in more than one zeolite. Common structural features include cages, channels, chains, and layers. The major difference from SBUs is that CBUs do not necessarily describe the entire framework, and that CBUs can overlap. CBUs offer a more pragmatic approach to highlight structural features, and that is perhaps why they are encountered more frequently in current literature.

For example, the **SOD** framework type can be built up using 6-rings only (its SBU), as can 50 other frameworks, but may be better described by its sodalite cage (its CBU). This cage is present in 11 different zeolite frameworks (most notably **FAU** and **LTA**). The sodalite cage is not an SBU, because it cannot be used to build up the **SOD** framework exclusively; T-atoms in the sodalite cages overlap in the **SOD** framework.

Historically, CBUs have been designated based on their usage. The big cage in **LTA** would be referred to as the α -cavity, whereas the small cage is the β -cage. The large cavity in **FAU** is usually referred to as the 'supercage', although this term is also used to describe large zeolite cages in general. Nowadays, common structural units are assigned a lower case italic three-letter code, as a means to communicate structural relationships between framework types. With the exception of double 4-rings (*d4r*), double 6-rings (*d6r*), and double 8-rings (*d8r*), each CBU is assigned a code corresponding to one of the framework types that they are featured in. Only CBUs that are present in two or more framework types are given a code. The α -cavity is characteristic for **LTA** and therefore designated *lta*, the β -cage is equivalent to the cage in **SOD**, and designated *sod*, and the supercage in **FAU** is not found in any other framework, and thus not given a code. Some CBUs are shown in Figure 2.5. At the time of writing, 58 CBUs were listed in the Database of Zeolite Structures, which can be found *via* framework type pages (Figure 2.2) by clicking on *List of all CBUs*. Notably, in general, these building units have no physical meaning, but simply serve as a means to describe a zeolite framework.

Several chains that are prevalent in a number of zeolite frameworks are shown in Figure 2.6. These are double zig-zag chain (*dzc*), double sawtooth chain (*dsc*), double crankshaft chain (*dcc*), Narsarsukite chain (*nsc*), and double Narsarsukite chain (*dnc*). Single chain versions of the first three double chains also exist, but they are so common that they are rarely seen as a defining structural feature.

Cages, cavities, or any other type of polyhedral unit can also be described by the number and kind of *n*-rings defining their faces (Figure 2.5). For example, a *d4r* unit and a *mor* unit both consist of eight T-atoms, but the former is made up of eight 4-rings, and is designated $[4^8]$, to distinguish it from the latter, which consists of four 5-rings, and is therefore designated $[5^4]$. A *sod* unit, whose surface is defined by six 4-rings, and eight 6-rings, would be designated as $[4^66^8]$. It is important to note the distinction between cages and cavities. The faces of a cage are all 6-rings or smaller (*e.g.* a *sod* cage), so they are inaccessible to guest molecules, whereas cavities have at least two faces that are larger than 6-rings (*e.g.* an *lta* cavity). These terms are often confused in the literature.

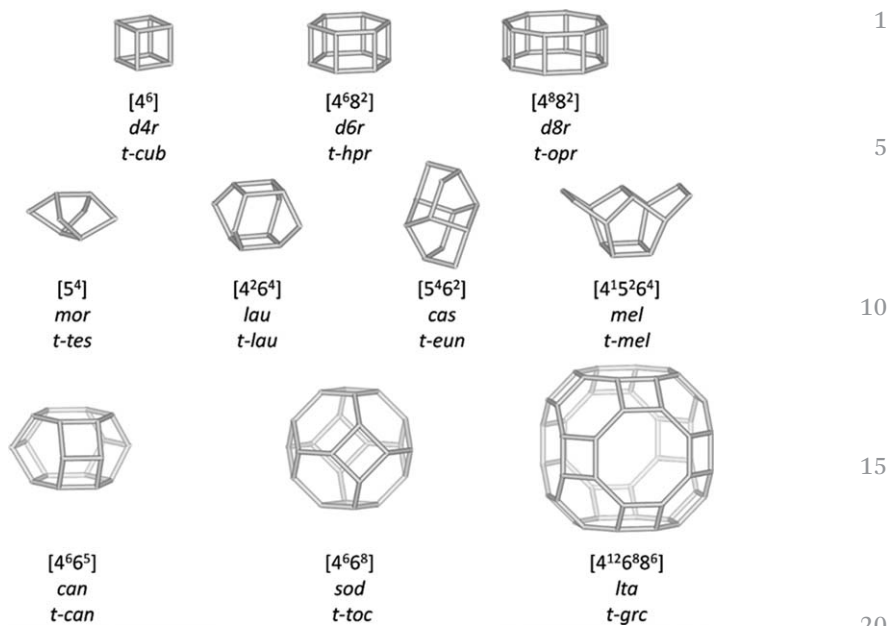


Figure 2.5 A selection of some of the most common CUBs, given by the corresponding face symbol, the CBU name, and the tile symbol, respectively.

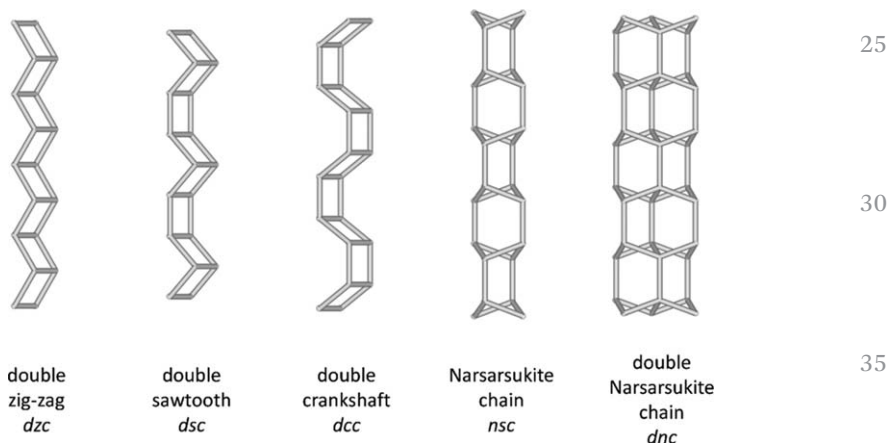


Figure 2.6 A selection of chains that have been found in several framework types.

A similar notation has been developed to describe two-dimensional layers or nets. Here, the number and kind of n -rings corresponding to each node are used. For example, **GIS** and **ABW** framework types can be described as different stackings of a layer consisting of 4-rings and 8-rings (Figure 2.7). Each node is part of one 4-ring and two 8-rings, forming a 4.8^2 net. The orientation of the fourth connection of the tetrahedron can be given as U (up) or D (down) to complete the three-dimensional description. The

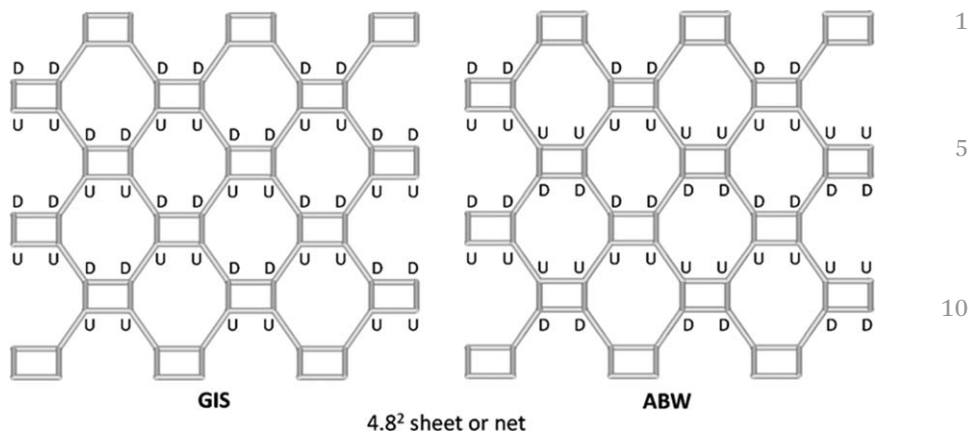


Figure 2.7 The 4.8^2 net that builds up both the GIS and ABW frameworks.

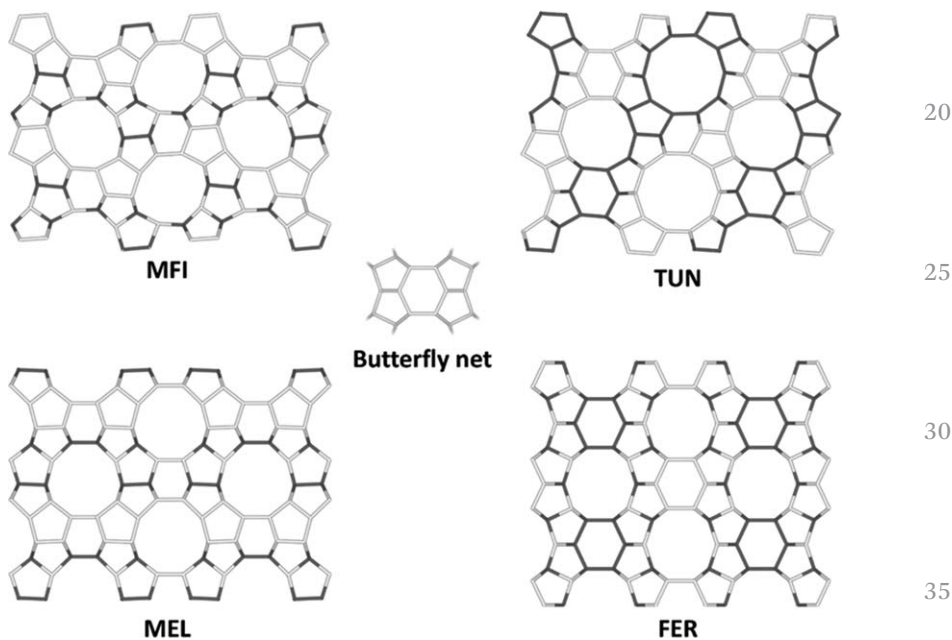


Figure 2.8 The butterfly net that builds up the MFI, MEL, TUN, FER, and many other frameworks. The T-atoms pointing up are in white and those pointing down are in black.

major difference between GIS and ABW is that the connections on one side of each 8-ring are all pointing up and the other half down (UUUDDDDD) for GIS, whereas for ABW the orientations are mixed (UUDDDUDDUU).

Many zeolite structures can be described using the same two-dimensional net/layer. One example is the butterfly net containing 5-, 6-, and 10-rings (Figure 2.8), which is found in 18 zeolite frameworks in the Database of Zeolite Structures; ten of them, *MRE, FER, MEL, SZR, MFS,

MFI, **TUN**, **IMF**, **BOG**, and **TON**, are built up solely from the butterfly net.² Different orientations of the TO_4 tetrahedra within the layer lead to different connectivities between neighboring layers, and thus different locations and orientations of the channels parallel to the layers. Some layers are corrugated and some are flat, resulting in different channel systems parallel to the layer.

Sometimes, zeolites that can be constructed from the same layer are referred to as polytypes. Polytypism is a special case of polymorphism, where crystal structures differ in one dimension only. Polytypes consist of identical layers, and differ only in the stacking sequence of these layers. Note the difference between polymorph and polytype. In a way, all zeolites composed of SiO_2 are polymorphs, but only a few are polytypes. For example, despite the fact that all of the ten framework types mentioned above consist of the same nets, only **MFI** and **MEL** are polytypes. The same is true for the ABC-6 family. Polytypism is found in the faujasite family (**EMT/FAU**), zeolite Beta (***BEA**), UTD-1 (**DON**), ITQ-39 (***-ITN**), ZSM-48 (***MRE**), SSZ-31 (***STO**), and more.³

2.2.5 Natural Tiles

One of the disadvantages of using SBUs or CBUs to describe zeolite frameworks is that their assignment is ambiguous and sometimes arbitrary. A large number of frameworks can be described in several ways, and CBUs sometimes overlap. Therefore, the idea of natural tilings has been extended to zeolites by Anurova *et al.*⁴ Tiles, sometimes referred to as natural building units (NBUs), divide Euclidean space, and are always *face-to-face*, which means that a face of a tile is shared by exactly two tiles. A tile is the interior of a generalized polyhedron that may contain divalent vertices and is topologically equivalent to a sphere.⁵

The main advantage is that the breakdown of a zeolite framework into its natural tiling is unambiguous, and can be done for any framework regardless of its complexity. One intrinsic feature of natural tiles is that they fill the entire space, unlike CBUs. The naming scheme for NBUs is slightly different from that of CBUs. They are given in italic typeface and prefixed with 't-' to avoid confusion. There are 121 tiles that occur more than once in the Database of Zeolite Structures. Figure 2.9 shows some of the most frequently

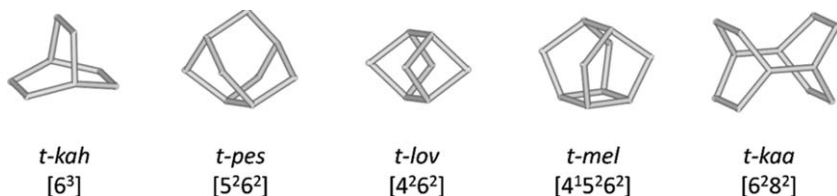


Figure 2.9 A selection of some of the most common tiles or natural building units (NBUs); *t-hpr*: *d6r*, *t-cub*: *d4r*, *t-tes*: *mor*, *t-can*: *can*, *t-lau*: *lau*. Nine more tiles are identical to CBUs and are given in Figure 2.5.

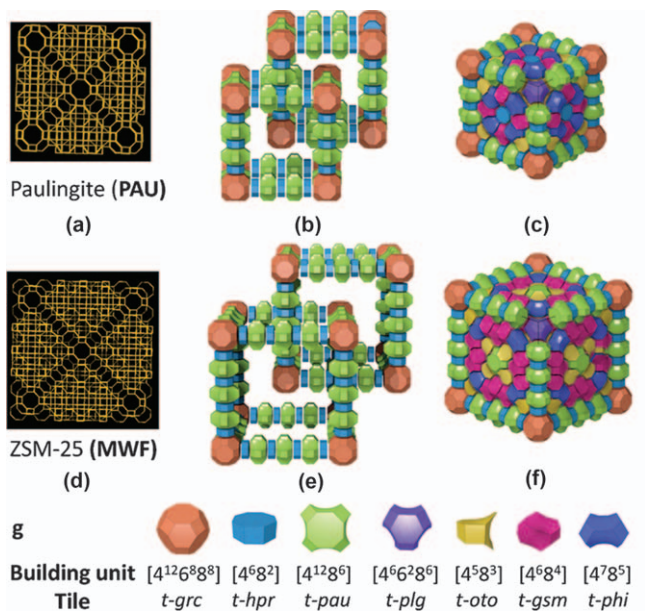


Figure 2.10 PAU (a–c) and MWF (d–f) frameworks represented using T–T connection (a, c) and tiling (c, f), respectively. Both frameworks are built from seven different tiles (g). While three of them (*t-grc*, *t-hpr*, *t-pau*) construct the unit cell edges, the other four (*t-plg*, *t-oto*, *t-gsm*, *t-phi*) are embedded in the space within the unit cell. PAU and MWF are two of the members in the zeolite RHO family with expanding unit cell and complexity, called a family of embedded isorecticular zeolite structures. Reprinted by permission of Macmillan Publishers Ltd: *Nature*,⁷ copyright (2015).

occurring natural tiles. Tilings can be generated by computer methods, *i.e.* using the program TOPOS.⁶

Tilings can be very useful to illustrate the channels and pores in zeolites, especially for complicated structures. An example is shown in Figure 2.10 for two complex and related zeolite structures, PAU and MWF (ZSM-25).⁷ Both zeolites contain intersecting 8-ring channels and are built up using the same types of tiles: *t-grc*, *t-hpr*, *t-pau*, *t-plg*, *t-oto*, *t-gsm* and *t-phi*.

2.2.6 Framework Density

The framework density (FD) for zeolites lies between 10 T-atoms per 1000 Å³ for low-density zeolites (such as –CLO, IRR, –IRY, –ITV, or RWY-type zeolites) up to 20–21 T-atoms per 1000 Å³ for high-density zeolites (such as AEN, CZP, JNT, MTF, MVY, PSI, or VET-type zeolites), whereas the minimum for dense tetrahedral framework structures is about 21 T-atoms per 1000 Å³. As a rule-of-thumb, FD offers a simple criterion for differentiating zeolites from dense tectosilicates.

2.2.7 Coordination Sequences

Coordination sequences (CSs) were first applied to zeolite frameworks by Meier and Moeck,⁸ who showed that they serve as a way of characterizing a framework numerically and uniquely in terms of consecutively neighbouring T-atoms. In a typical zeolite framework, every T-atom is connected to $N_1 = 4$ neighbouring T-atoms (the first ‘shell’). Each of these is in turn connected to a maximum of three new T-atoms, and thus $N_2 \leq 12$ for the second shell. It follows that:

$$N_0 = 1, N_1 = 4, N_2 \leq 12, N_3 \leq 36, N_4 \leq 108, N_k \leq 4 \cdot 3^{k-1}$$

CSs are calculated for every unique atom in a framework, and are independent of the unit cell and crystallographic symmetry. This makes them ideally suited as a fingerprint for identifying and classifying zeolite framework types. CSs are typically computed up to the tenth shell. Sometimes calculation of higher shells is necessary to describe a framework uniquely, as is the case when comparing **LTA** and **RHO**. Examples for **LTA**, **RHO**, **SOD**, **FAU**, and **EMT** are given in Table 2.1.

2.2.8 Vertex Symbols

A vertex symbol is a geometrical shorthand used to represent the vertices of a tiling as a sequence of faces around the given vertex, first used in connection with zeolite-type networks by O’Keeffe and Hyde.⁹ A vertex symbol is a sequence of integers representing the smallest n -rings the T-atom is part of. Every 4-connected T-atom is part of six n -rings, and therefore the vertex symbol has the notation ‘ $a.b.c.d.e.f$ ’. The order is determined by the size of the n -rings, where opposing faces are grouped together. For example, **SOD** has the vertex symbol $4 \cdot 4 \cdot 6 \cdot 6 \cdot 6 \cdot 6$, indicating that its T-atom has two opposing 4-rings, and two pairs of opposing 6-rings. For **LTA**, the vertex symbol is $4 \cdot 6 \cdot 4 \cdot 6 \cdot 4 \cdot 8$, indicating two pairs of opposing 4- and 6-rings, and one pair with a 4-ring and an 8-ring. A subscript is used to indicate that a face is ambiguous, e.g. 6_2 or 8_2 , or an asterisk (*) in the case where no ring is formed.

Just like coordination sequences, vertex symbols offer a way of describing symmetrically independent T-atoms that characterize a zeolite framework type, and the two are often used together as a unique identifier. For example,

Table 2.1 Coordination sequences and vertex symbols for five framework types.

FTC	ATOM	Coordination sequences, N_1 to N_{10-12}	Vertex symbol
LTA	T ₁	4 9 17 28 42 60 81 105 132 162	$4 \cdot 6 \cdot 4 \cdot 6 \cdot 4 \cdot 8$
RHO	T ₁	4 9 17 28 42 60 81 105 132 162	$4 \cdot 4 \cdot 4 \cdot 6 \cdot 8 \cdot 8$
SOD	T ₁	4 10 20 34 52 74 100 130 164 202	$4 \cdot 4 \cdot 6 \cdot 6 \cdot 6 \cdot 6$
FAU	T ₁	4 9 16 25 37 53 73 96 120 145	$4 \cdot 4 \cdot 4 \cdot 6 \cdot 6 \cdot 12$
EMT	T ₁	4 9 16 25 37 53 73 96 121 148 178 212	$4 \cdot 4 \cdot 4 \cdot 6 \cdot 6 \cdot 12$
	T ₂	4 9 16 25 37 53 73 96 121 148 179 214	$4 \cdot 4 \cdot 4 \cdot 6 \cdot 6 \cdot 12$
	T ₃	4 9 16 25 37 53 73 97 124 152 180 210	$4 \cdot 4 \cdot 4 \cdot 6 \cdot 6 \cdot 12$
	T ₄	4 9 16 25 37 53 73 96 120 145 174 210	$4 \cdot 4 \cdot 4 \cdot 6 \cdot 6 \cdot 12$

while LTA and RHO have identical CS up to the tenth shell, their vertex symbols are different; $4 \cdot 6 \cdot 4 \cdot 6 \cdot 4 \cdot 8$ and $4 \cdot 4 \cdot 4 \cdot 6 \cdot 8 \cdot 8$, respectively (Table 2.1). Unlike CS, vertex symbols are also useful for determining the smallest rings present in a zeolite framework.

2.3 Zeolite Structures

Although zeolites with the same framework type may share a number of physical properties, such as framework density, channel dimensionality, and pore volume, other properties should also be considered. Zeolite structures in real materials are characterized by the framework composition, location of extra-framework cations, molecules or organic species absorbed in the pores, and stacking faults or defects.

2.3.1 Framework Composition

The framework composition can be considered to be the *decoration* of the zeolite framework. The location of heteroatoms can alter the performance of materials with the same framework type for a particular application significantly. Many elements, such as Ge, B, Al, Ga, Zn, Be, P, and transition metals such as Fe, Co, or Ti, can be inserted into some of the T-sites. Even a small amount can have profound effects on the performance, properties, and/or catalytic selectivity of a material. These elements are often not ordered, and usually only partially occupy a T site, sharing it with Si.

For example, the range of Si/Al ratio varies from zeolite to zeolite. Some zeolites, such as ZSM-5 are strictly high silica ($\text{Si/Al} > 12$), whereas other zeolites, such as synthetic faujasite (zeolite X/Y), can be prepared in both high silica and high alumina forms (typically $1.2 \leq \text{Si/Al} \leq 3.0$). Zeolite A is an example of a zeolite that is prepared with equal amounts of Si and Al ($\text{Si/Al} = 1$). Because Al–O–Al bonds are unlikely to occur,¹⁰ Si and Al tetrahedra are strictly alternating in zeolite A. The inclusion of Al in a silicate framework introduces a net negative charge into the framework, which is balanced by counterions, such as Na^+ or protons (H^+). Zeolites with a low Si/Al ratio offer possibilities for ion exchange, while zeolites with a high Si/Al ratio can act as a Brønsted acid when H^+ are present as counterions.

Aluminophosphates (AlPOs) are neutral framework materials consisting of strictly alternating Al and P tetrahedra, and therefore no odd-numbered rings (such as 5-rings) occur in their framework structures. AlPOs have been prepared with more than 40 different framework types, and can be made anionic in a similar way to pure silicates *via* the introduction of heteroatoms. In a silicoaluminosilicate (SAPO), Si substitutes preferably into P sites, and introduces a local negative charge, similar to Al in aluminosilicates.

The framework composition also has an indirect effect on the framework structure. High-silica zeolites are rich in 5-rings. Aluminosilicates are known to contain double crankshaft chains, but in aluminophosphates Narsarsukite chains are more common. The inclusion of germanium promotes the formation of double 4-rings, and beryllo- or zincosilicates are more likely to

contain 3-rings. Materials with strictly alternating sites, such as aluminosilicates with Al/Si = 1, aluminophosphates, and gallophosphates, require the presence of even-numbered rings, and are therefore devoid of odd-numbered rings.

2.3.2 Extra-framework Species

Besides the framework type and composition, the pore content is also of interest. A significant amount of early research effort was focused on the distribution of extra-framework species and cations in the zeolite channels and cavities, because these strongly affect the physicochemical properties of a material and have an impact on its ion-exchange capacity, catalytic selectivity, and adsorptive qualities. The cations can usually be found in only a few distinct crystallographic sites, and common sites are labelled based on their usage. The *Compilation of Extra Framework Sites in Zeolites* in 1982¹¹ includes this information for 36 framework types. The large number of entries for the framework types **FAU** (69), **LTA** (62), and **MOR** (13) is an indication of the importance of these materials, as well as the attention that the type and location of the cation in these materials received. In the *Compilation*, locations are categorized (A, B, C, etc.). For example, the ferrierite zeolite family (**FER**) consists of three very similar species: ferrierite-Mg, ferrierite-Na, and ferrierite-K, based on the dominant cation in the A location. That said, there is no standard way of describing these positions, and sometimes $\alpha/\beta/\gamma$ or a designation based on the channel or cage is used. For example, for **FAU**, sites are consistently labelled I, I', II, II', or III in the literature.

Equally important is the location of the organic structure-directing agent (OSDA) in the channel system. It is well known that the organic guest molecules introduced into a zeolite synthesis gel play a key role as OSDA and can have a profound effect on the microporous system that results. As early as 1969, Baerlocher and Meier performed a structural analysis using powder X-ray diffraction (PXRD) data collected on a synthetic sodalite material¹² and on Na-P1^{13,14} to locate tetramethylammonium (TMA) within the cages. However, the real breakthrough was the location of the tetrapropylammonium (TPA) ion in the channel system of ZSM-5^{15,16} using single-crystal X-ray diffraction data. The location of the OSDA within the channel system has played an important role in understanding zeolite synthesis and in providing detailed coordinates against which theoretical molecular modelling of the host-guest interactions can be validated.¹⁷ The latter have allowed researchers to target specific zeolite structures and properties, and constitutes a first step in the direction of the rational design of zeolite syntheses.¹⁸

2.3.3 Stacking Faults and Disorder

In the ideal case, zeolite structures can be described in terms of a neatly ordered, repeating framework. However, intergrowths, stacking faults, and

other sorts of disorder are regularly observed in zeolites, particularly those with layered structures and germanosilicates. For example, the **MEL** and **MFI** framework types are closely related, as both consist of *pentasil* layers. The only difference is in the way adjacent layers are related to one another (a mirror plane in **MEL** and a centre of inversion in **MFI**). At any point, a stacking fault may occur in the arrangement of the layers. If substantial domains of two different framework types share a common phase, this material is referred to as an intergrowth.

Examples of zeolites and zeolite families containing stacking disorders include zeolite beta (***BEA**), **FAU/EMT**, **SSZ-26/SSZ-33 (CON)**, the **ABC-6** family, **ZSM-48 (*MRE)**, **SSZ-31 (*STO)**, **ZSM-5/ZSM-11 (MFI/MEL)**, and **ITQ-39 (*-ITN)**.¹⁹ Zeolites can also have some local disorders in the framework. Recent examples of zeolites containing such local disorders include **EMM-23 (*EMT)**,²⁰ **SSZ-57 (*SFV)**,²¹ and **SSZ-61 (*-SSO)**.²² For further information on stacking disorder in zeolites and open-frameworks, the reader is referred to a recent review on this topic.³

Disorder makes the analysis of these zeolites challenging, and there is no standard way to characterize the structure of a disordered zeolite material. Stacking faults are typically described qualitatively by means of high-resolution electron microscopy images. The program **DiFFaX**²³ can be used to simulate powder X-ray and neutron spectra, and single-crystal electron diffraction patterns of faulted materials, and was developed specifically to characterize zeolites. Alternatively, the programs **DISCUS**,²⁴ **FAULTS**,²⁵ and **TOPAS**²⁶ allow the user to refine the stacking disorder against powder diffraction data directly.

2.4 Examples of Framework Structures

2.4.1 SOD

Type material: sodalite, $[\text{Na}_8\text{Cl}_2][\text{Al}_6\text{Si}_6\text{O}_{24}]$ -**SOD**

The **SOD** framework type can be described as a body-centred cubic arrangement of face-sharing *sod* units or β -cages (Figure 2.11). Adjacent cages are connected *via* 6-rings only, so **SOD** lacks any sort of channel system, and this significantly limits its sorption capacity. However, the *sod* units have a free diameter of approximately 6.3 Å, giving **SOD** a framework density of approximately 17.2 T/1000 Å³, which is fairly average for zeolites. An alternative way of describing the **SOD** framework is as an ABCABC stacking of 6-rings along the $\langle 111 \rangle$ direction (body diagonal), making it a part of the **ABC-6** family.

2.4.2 LTA

Type material: Linde type A (zeolite A), $[\text{Na}_{12}(\text{H}_2\text{O})_{27}]_8[\text{Al}_{12}\text{Si}_{12}\text{O}_{48}]_8$ -**LTA**

The **LTA** framework type describes a small-pore zeolite with mutually perpendicular, straight channels forming a three-dimensional channel

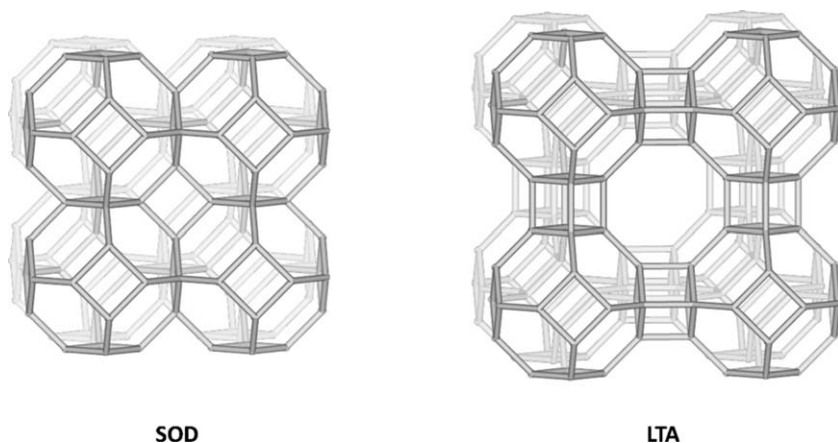


Figure 2.11 SOD and LTA framework types.

system (Figure 2.11). At the channel intersection is the *lta* or α -cavity. The **LTA** framework is related to that of **SOD**, and can be described with a primitive cubic arrangement of *sod* units. The major difference is that the interfacing 4-rings of **SOD** are replaced by double 4-rings (*d4rs*), forming an *lta* unit in the centre position. Alternatively, **LTA** can be described as a primitive cubic arrangement of *lta* units, each of them connected to six neighbouring cages *via* 8-ring openings, with a *sod* unit in the centre. The **LTA** framework type is a very open one with a framework density of 12.9 T-atoms per 1000 Å³. This allows zeolite A to absorb a large amount of water, which is why it is used as an industrial desiccant.

LTA type zeolites come in a large number of flavours, and significant structural modifications are reflected in the name of the zeolite. For example, the openings to the *lta* units in zeolite A are defined by 8-rings, roughly 4.1 Å in diameter, but these can be influenced by the presence of charge-balancing cations, such as Na/K, Na, or Na/Ca. These result in zeolites 3A, 4A, and 5A, respectively, where the number refers to the approximate pore size in Å. If a zeolite A material is used for ion-exchange purposes, the exchanged ion can be used as a prefix, *e.g.* its sodium form is given as zeolite NaA and its potassium form as zeolite KA. Zeolites from the **LTA** family are produced on a massive scale for their superior ion-exchange performance, and are primarily used as water softeners in laundry detergents.

2.4.3 FAU

Type material: faujasite, $[(\text{Ca}^2, \text{Mg}^2, \text{Na}_2)_{29}(\text{H}_2\text{O})_{240}][[\text{Al}_{58}\text{Si}_{134}\text{O}_{384}]\text{-FAU}$

Just like **LTA**, the **FAU** framework type can be built up from *sod* units. However, in this case, the 6-rings of the neighbouring *sod* units are facing one another, and are connected *via* oxygen bridges to form shared double

6-rings (*d6rs*; Figure 2.12). This creates a diamond cubic lattice arrangement of *sod* units. That is, the *sod* units follow the same arrangement as the carbon atoms in the diamond structure. This creates a large open framework structure, with a very low framework density of 12.7 T-atoms per 1000 Å³, in part due to the large ‘supercage’ ([4¹⁸6⁴12⁴]) at the channel intersection (Figure 2.13). **FAU** has a three-dimensional channel system along the ⟨110⟩ direction, with 12-ring openings. The **FAU** framework type can be described as puckered hexagonal layers stacked in an ABCABC arrangement. Materials with the **FAU**-type, such as zeolite Y, can be produced cheaply with a wide range of Si/Al. In addition, they have high thermal stability, a large void volume of about 50%, and applications as a cracking catalyst, and are therefore widely used in industrial applications.

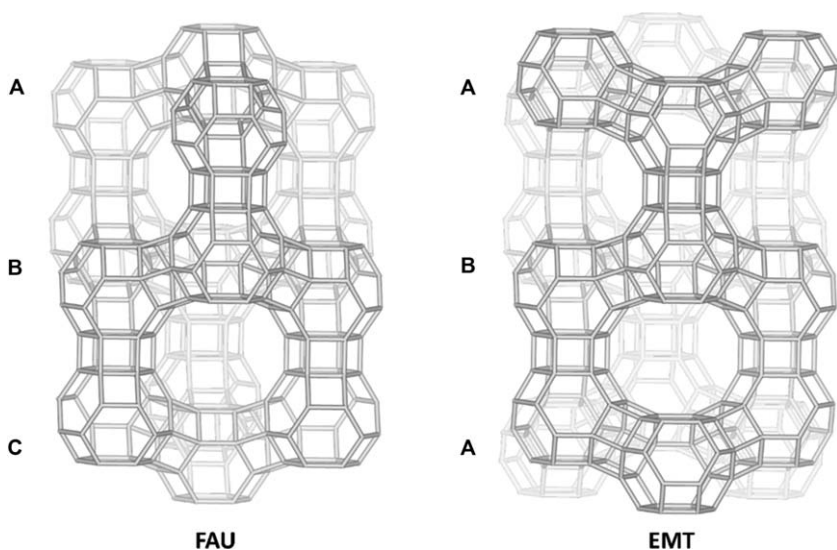


Figure 2.12 FAU and EMT framework types.

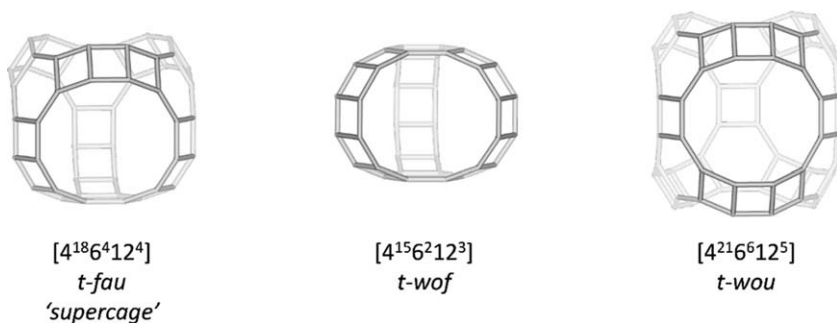


Figure 2.13 Supercage found in **FAU** (*t-fau*), and the medium and large cage of **EMT** (*t-wof* and *t-wou*, respectively).

2.4.4 EMT

Type material: EMC-2, $|\text{Na}_{21}(\text{C}_{12}\text{H}_{24}\text{O}_6)_4|[\text{Al}_{21}\text{Si}_{75}\text{O}_{192}]$ -EMT

The **EMT** framework is very similar to that of **FAU**, because it is also built up of *sod* units that are connected *via* oxygen bridges extruding from the 6-rings, but the arrangement of these units is slightly different. While the *sod* units are all oriented in the same way for **FAU**, for **EMT** they are rotated by 30° around the vertical axis from layer to layer (*i.e.* the orientations of some of the 4- and 6-rings are reversed). The framework of **EMT** can also be described using the same puckered hexagonal layer as found in **FAU**. **EMT** can be described as an ABAB stacking of hexagonal layers that are related to one another *via* a mirror plane. In Figure 2.12, the B-layers in both frameworks are equivalent. **EMT** has two distinct supercages, a smaller one with three 12-ring openings ($[4^{15}6^212^3]$), and a larger one with five 12-ring openings ($[4^{21}6^612^5]$; Figure 2.13). The channel system of **EMT** is three-dimensional, with a 12-ring channel along the $[001]$ direction, perpendicular to 12-ring channels in the plane normal to $[001]$. **EMT** is the hexagonal analogue of **FAU**, in the same way that lonsdaleite is the hexagonal analogue of diamond. Because of their structural similarity, intergrowths of **EMT/FAU** are known to occur.²⁷ Like **FAU**, **EMT** type materials are also well-suited for catalytic applications.

2.4.5 RHO

Type material: Rho, $|\text{(Na,Cs)}_{12}(\text{H}_2\text{O})_{44}|[\text{Al}_{12}\text{Si}_{36}\text{O}_{96}]$ -RHO

The **RHO** framework type can be described as a primitive cubic arrangement of *lta* units, similar to how **SOD** is described using *sod* units. The 8-rings of adjacent *lta* units are joined *via* oxygen bridges to form a double 8-ring (*d8r*) between them (Figure 2.14). **RHO** contains two identical, but

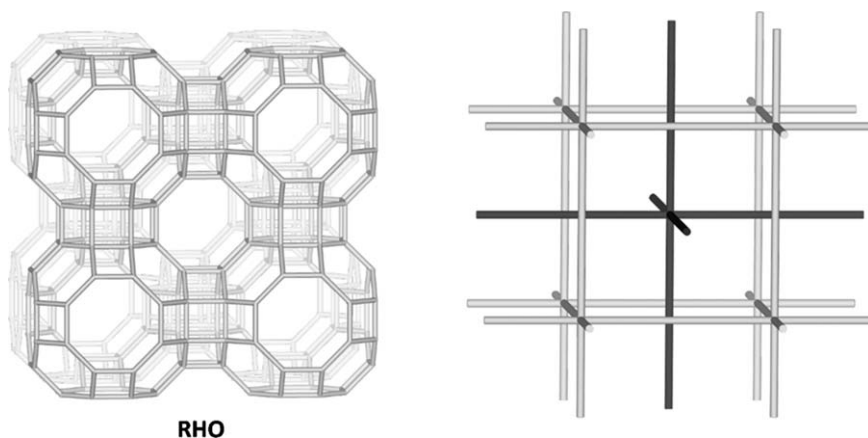


Figure 2.14 RHO framework type and its channel system.

non-intersecting three-dimensional channel systems with mutually perpendicular 8-ring channels.

2.4.6 MOR

Type material: mordenite, $[\text{Na}_8(\text{H}_2\text{O})_{24}][\text{Al}_8\text{Si}_{40}\text{O}_{96}]$ -**MOR**

The structure of **MOR** can be described in terms of chains of edge-sharing *mor* units ($[\text{5}^4]$) along the [001] direction (Figure 2.15). Alternating mirror images of these chains connected *via* oxygen bridges form puckered layers containing circular 8-ring pores perpendicular to the [010] direction. Alternating layers, each shifted by a translation of $1/2c$ compared to its neighbour, once again connected *via* oxygen bridges, complete the three-dimensional framework structure. This creates alternating, ellipsoidal 8- and 12-ring channels between the layers. Although this results in a two-dimensional channel network, the 8-rings connecting the large 12-ring channels are displaced with respect to one another, and this throttles diffusion between the channels. As a consequence, **MOR** effectively has a one-dimensional channel system. Synthetic mordenite is used in the petrochemical industry for acid-catalysed isomerization of alkanes and aromatics.

2.4.7 MFI

Type material: ZSM-5, $[\text{Na}_n(\text{H}_2\text{O})_{16}][\text{Al}_n\text{Si}_{96-n}\text{O}_{192}]$ -**MFI**, $n < 27$

For a long time (since 1978), **MFI**, with its 12 unique T-atoms, was the most complex zeolite framework structure known, until the structure of SSZ-23 (**STT**) with 16 unique T-atoms was reported in 1998. Although it is possible to describe the framework structure of **MFI** using *mor* units ($[\text{5}^4]$), it is easier to do so in terms of *mfi* units ($[\text{5}^8]$, sometimes referred to as *pentasil*

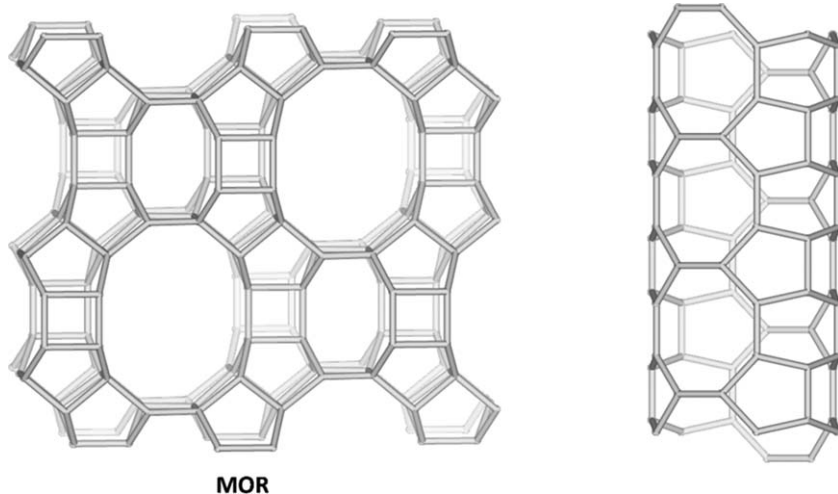


Figure 2.15 MOR framework type and its 12-ring channel.

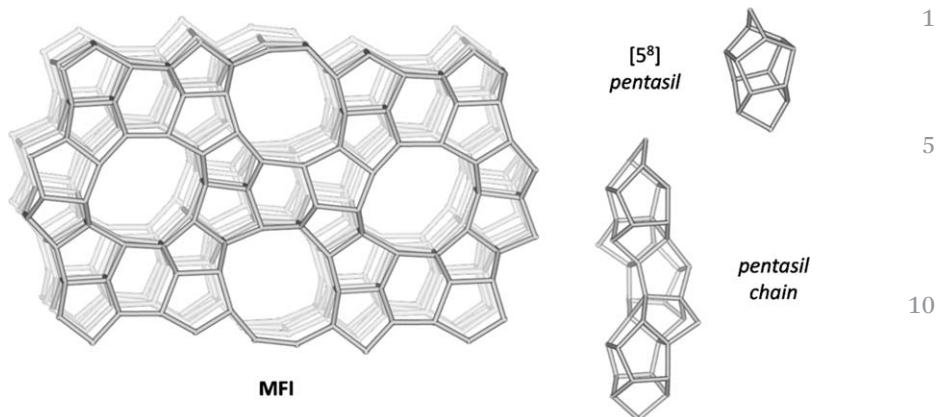


Figure 2.16 MFI framework type and its 10-ring channel. Pentasil units are linked to form the pentasil chains that form the basis of the MFI framework type.

units) that are linked to form *pentasil* chains. These chains are mirrored perpendicular to the *b*-axis to form corrugated layers with 10-ring pores in the *bc*-plane (Figure 2.16). Adjacent layers are related to one another *via* an inversion centre and linked *via* oxygen bridges. This results in a framework with straight channels along [010], and sinusoidal channels along [100] (perpendicular to the layers). Despite the lack of channels along the [001] direction, the combination of straight and sinusoidal channels results in a three-dimensional channel network. The MEL framework type is related to MFI in that it is made up of the same layers. However, adjacent layers are related to one another by a mirror plane instead of an inversion centre, producing straight 10-ring channels in both directions. Intergrowths of MFI and MEL are known to exist, and have been well studied.^{28,29}

Because ZSM-5 has proven to be one of the most useful zeolites for the petrochemical industry, a large number of variations with the MFI framework type have been synthesized. This serves as an excellent example of how the chemistry of a zeolite influences its properties. For example, ZSM-5 is a high silica aluminosilicate, and is used for acid-catalysed reactions such as hydrocarbon isomerization and the alkylation of hydrocarbons. The MFI framework type has also been produced as a pure silicate (silicate-1), which is used as a molecular sieve, and as a titanosilicate (TS-1), which is a catalyst for selective oxidation reactions under mild conditions using hydrogen peroxide as the oxidant.

2.4.8 FER

Type material: ferrierite, $|\text{Mg}_2\text{Na}_2(\text{H}_2\text{O})_{18}|[\text{Al}_6\text{Si}_{30}\text{O}_{72}]$ -FER

The FER framework can be described in terms of layers consisting of edge-sharing *mor* units, that are interconnected *via* oxygen bridges to form

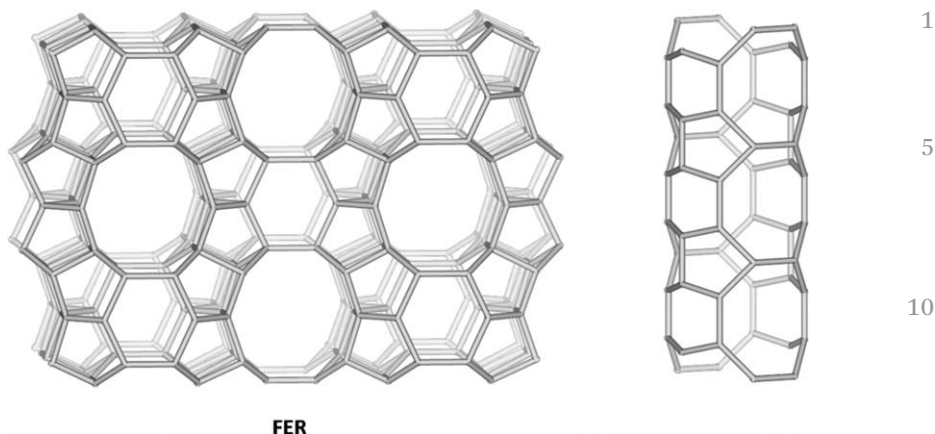


Figure 2.17 FER framework type and its 10-ring channel.

alternating 6-ring and 10-ring channels along the $[001]$ direction. This makes the projection along this axis very similar to that of **MFI**. For **FER**, however, straight 8-ring channels run along $[010]$ and intersect the 10-ring channels to form a two-dimensional channel network (Figure 2.17). The region connecting parallel 10-ring channels is defined by small cavities ($[5^8 6^6 8^2]$) that are only accessible through the small 8-ring pores. Materials with the **FER** framework structure can be synthesized with a great variety of cations, and are therefore exploited as catalysts, as well as filters and ion-exchange agents.

2.4.9 CHA

Type material: chabazite, $[\text{Ca}_6(\text{H}_2\text{O})_{40}][[\text{Al}_{12}\text{Si}_{24}\text{O}_{72}]]\text{-CHA}$

The **CHA** framework type can be described as a hexagonal array of double 6-ring units with an ABCABC stacking arrangement, or as an AABBC-CAABBCC stacking of 6-ring units, making it a part of the ABC-6 family. Each double 6-ring is connected to six other 6-rings *via* oxygen bridges forming 4-rings between them (Figure 2.18). **CHA** contains large, elongated cavities that are easily accessible from adjacent cavities *via* six 8-rings, thus forming a three-dimensional channel system.

CHA can be produced as a silicoaluminophosphate (SAPO-34) or high silica aluminosilicate (SSZ-13). The small pores combined with large internal surface area and good thermal stability make **CHA** type materials suitable for DeNoX catalysis (with Cu or Fe) and for MTO conversion, and as membranes for gas separations.

2.4.10 MWW

Type material: MCM-22, $[\text{H}_{2.4}\text{Na}_{3.1}][[\text{Al}_{0.4}\text{B}_{5.1}\text{Si}_{66.5}\text{O}_{144}]]\text{-MWW}$

MWW is a layered framework, where each layer can be viewed as two sub-layers consisting of a hexagonal array of $[4^3 5^6 6^3]$ units sharing 4-ring faces.

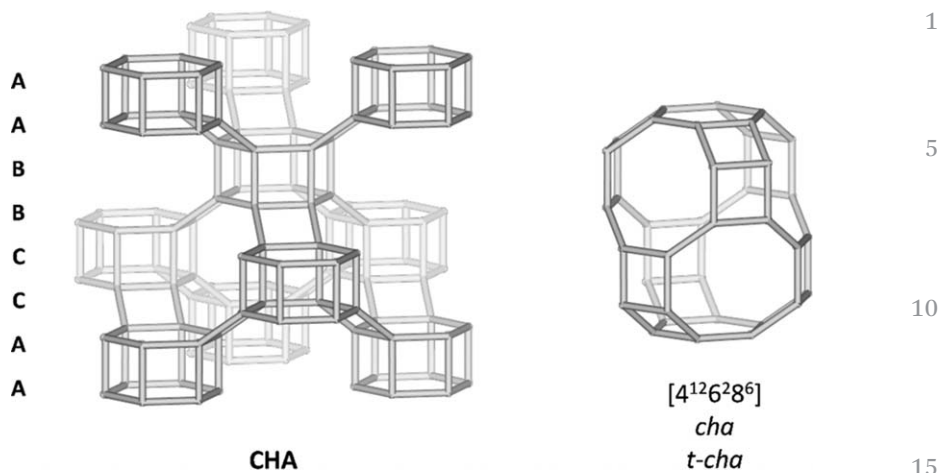


Figure 2.18 CHA framework type and its cavity.

The sub-layers are mirrored, and connected *via* oxygen bridges, creating double 6-rings, to form the larger layer. Each layer contains an isolated, two-dimensional 10-ring channel network. The layers are stacked, and connected *via* single oxygen bridges, creating another two-dimensional 10-ring channel network. This results in a rather unusual channel system, consisting of two non-intersecting, alternating, independent two-dimensional networks, one within the layer and one between the layers. The latter also features large 12-ring side-pockets (Figure 2.19).

The first material discovered with the **MWW** framework type, MCM-22, was synthesized *via* an intermediate layered precursor (MCM-22P), and later directly as MCM-49. This prompted researchers to investigate new materials consisting of **MWW** layers. A large number of different spatial arrangements of these layers has now been realized, either *via* direct synthesis of expanded or disordered forms or *via* post-synthesis treatment, such as pillaring, delamination, or stabilization in expanded form.³⁰

2.4.11 *BEA

Type material: Beta polymorph A, $[\text{Na}_7][\text{Al}_7\text{Si}_{57}\text{O}_{128}]^-$ *BEA

The structure of zeolite beta (*BEA) is difficult to describe. The three-letter code in the Database of Zeolite Structures is prefixed with an asterisk (*) to indicate that it is disordered. The framework described corresponds to an end member (polymorph A) of a polytypic series of structures that belong to the zeolite beta family of structures. No ordered material with the *BEA framework type has yet been produced.

Zeolite beta can be described in terms of *mor* units that are linked together *via* 4-rings to form a layer with saddle-shaped 12-rings. The layers are consistent between the different polymorphs of zeolite beta. The disorder arises

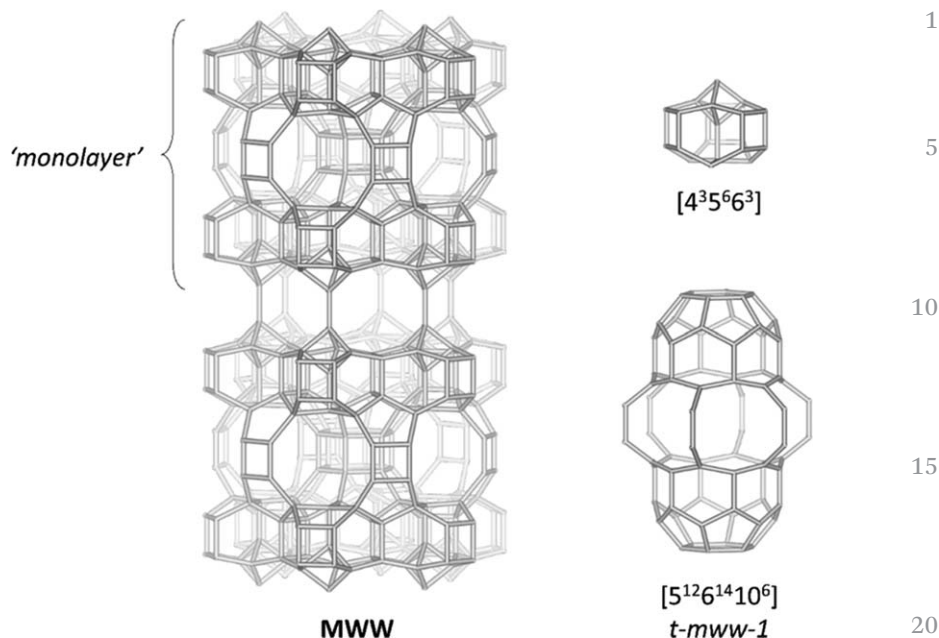


Figure 2.19 MWW framework type showing the monolayer, the small cage, and a pair of side pockets that are accessible from the interlayer channel.

from the way these layers are stacked. In polymorph A, adjacent layers are related to one another by a clockwise 90° rotation around its crystallographic four-fold screw axis, resulting in a chiral but ordered structure (Figure 2.20). Its enantiomorph is produced by maintaining an anticlockwise 90° rotation throughout the crystal. The disordered structure of zeolite beta emanates when random sequences of clockwise and anticlockwise rotations are mixed. Despite the stacking sequence, the channel system is always three-dimensional with 12-ring pores.

In another end member of the zeolite beta family, termed polymorph C, the layers are stacked with strictly alternating clockwise and anticlockwise rotations of the layers. Zeolite beta polymorph C contains double 4-rings, and was initially synthesized as a pure germanate.³¹ Because that structure is ordered, it was assigned its own code, **BEC**.

Because zeolite beta can be synthesized with a very broad range of chemical compositions and has a 3D 12-ring channel system, it has found many applications in petrochemistry, fine chemistry, biomass transformation, and environmental chemistry.

2.4.12 *–SSO

Type material: SSZ-61, $[(C_{16}H_{26}N)_4][Si_{80}O_{160}(OH)_4]$ *–SSO

The framework of *–SSO is characterized by large one-dimensional, dumbbell-shaped, 18-ring channels running along the [010] direction

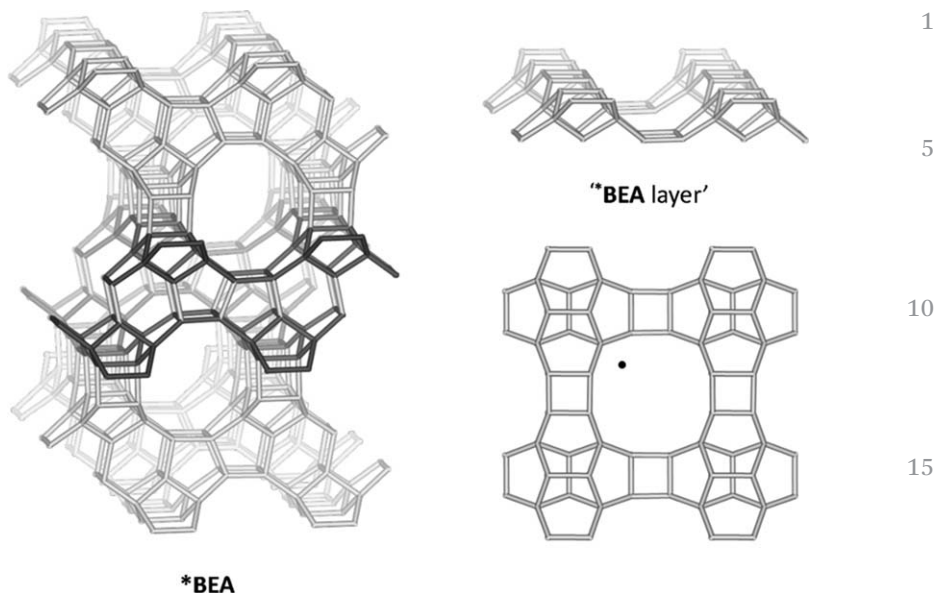


Figure 2.20 *BEA framework type with two layers highlighted. The layer is shown separately from two projections, with the screw axis indicated by a dot (normal to the plane of projection) that relates adjacent layers.

(Figure 2.21). T-atoms at the waist of the channel are only three-connected and bonded to terminal O atoms pointing into the channel, essentially dividing the channel into two parts.

This framework nicely illustrates how a family of zeolites can be built up from the same starting layer.

The *–SSO framework structure is closely related to that of MTW, and SFN (Figure 2.21). All three consist of the same *mtw* layers; they differ only in the connection between these layers. In MTW the layers are connected directly, creating single zigzag chains running down the sides of the 12-ring channel. In SFN, the layers are separated by 4-rings, which increases the *c*-axis by 2.9 Å and creates a 14-ring channel with double zigzag chains. In *–SSO, the connection is *via* two 5-rings, extending the axis by 7.7 Å and creating an 18-ring channel with triple zigzag chains. The three chains are linked in an alternating fashion to form a series of 6-rings. Pairs of adjacent 6-rings are bridged *via* two T-atoms to form *mor* units on both sides of the chains. These two T-atoms are only three-connected, and this results in two terminal O atoms protruding into the 18-ring channel. Intergrowths of *–SSO and MTW have been observed by high-resolution transmission electron microscopy.³

In SSZ-61, the type material of *–SSO, a minor source of disorder involving the three-connected T-atoms, was identified. These T-atoms are linked in a pairwise fashion, but two pairing arrangements are possible. In SSZ-61, these arrangements are not necessarily in register from one chain to the next.

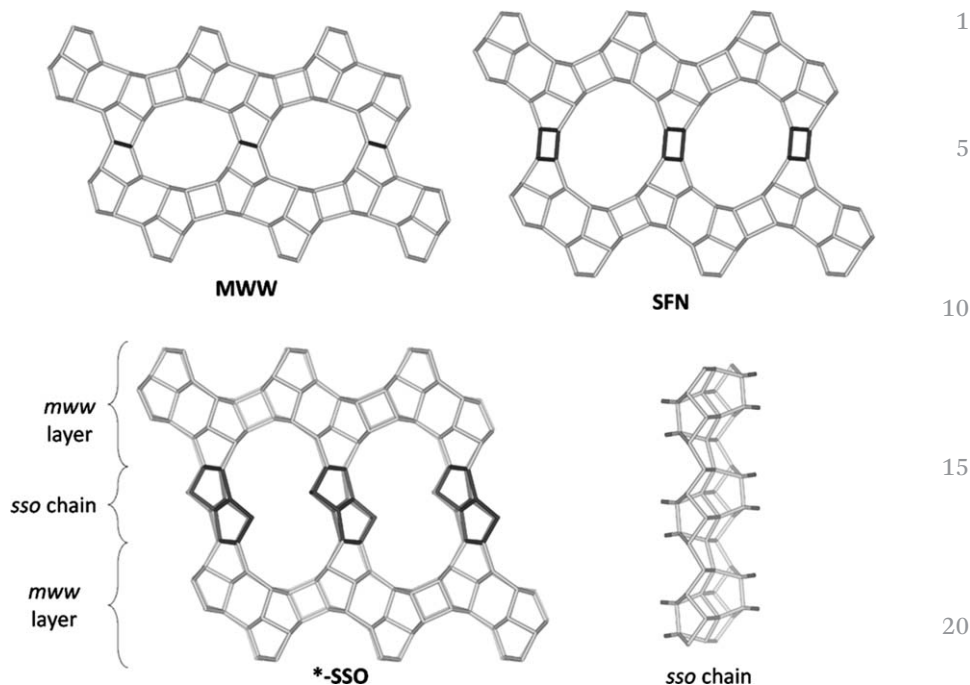


Figure 2.21 Comparison of the MWW, SFN, and *-SSO frameworks, viewed along their 12-, 14-, and 18-ring channels, respectively, with the chains connecting the *mww* layers in each framework highlighted. The *sso* chain connects the *mww* layers in the *-SSO framework, and has terminal O atoms (shown in red).

2.4.13 UTL

Type material: IM-12, $[\text{Ge}_{13.8}\text{Si}_{62.2}\text{O}_{152}]$ -UTL

The UTL framework type can be described as layers containing primarily 5-rings. The layers consist of alternating chains of $[4^{15^8}]$ (*non*) units that are linked together *via* oxygen bridges and an additional T atom. The layers themselves are connected *via* *d4r* units to form a two-dimensional network of perpendicular 12- and 14-ring channels (Figure 2.22).

Germanium is known to play a stabilizing role in the formation of *d4r* units in germanosilicates,³²⁻³⁴ promoting the formation of novel zeolites. However, the incorporation of Ge into a zeolite framework typically leads to a reduction in thermal and hydrothermal stability. Researchers have found ways to turn this drawback into an advantage and proposed a novel strategy to transform a preformed known zeolite into new zeolite framework types, which has been successfully demonstrated using the germanosilicate IM-12 (UTL).^{35,36} The structure of IM-12 is built up of Ge-rich *d4r* units that connect the Si-rich layers. The Ge in the *d4r* units can be selectively removed under the right conditions. In this way the layers can be rearranged and connected into a new framework. These synthesis strategies have been used for the

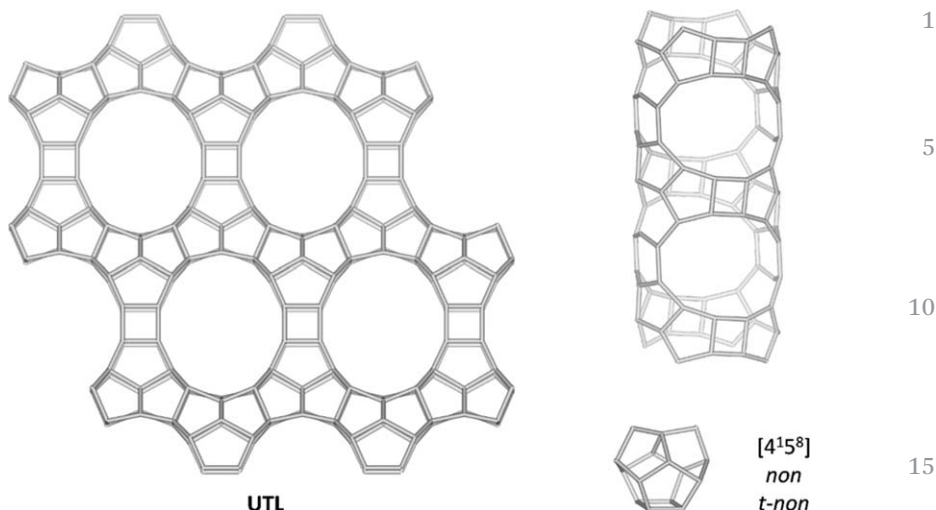


Figure 2.22 UTL framework type viewed along the 14-ring channel, and its 14-ring channel.

preparation of new high silica zeolite framework structures that are inaccessible through traditional, hydrothermal synthesis.^{36–38}

2.4.14 Zeolite Frameworks with Extra-large Pores

Zeolites with extra-large pores (>12-ring) are less common. Among the 232 zeolite framework types in the Database of Zeolite Structures, only 18 have extra-large pores; 11 of them have ring sizes ≥ 16 . These are 30-ring ($-ITV$),³⁹ 21–24-ring ($*-EWT$), 20-ring ($-CLO$ and $-IFU$), 18-ring (ETR , IRR , ITT , $*-SSO$, VFI) and 16-ring (IFO and $-IRY$); five of them are germanosilicates ($-ITV$, $-IFU$, IRR , ITT , and $-IRY$) with $d4r$ units.

The germanosilicate ITQ-37 ($[(CN_2H_4)_3(H_2O)_{10.5}][Ge_{80}Si_{112}O_{400}H_{32}F_{80}]$) with the $-ITV$ framework contains 30-ring gyroidal channels, and is one of the few chiral zeolites (Figure 2.23).³⁹ The framework and channel systems have opposite chirality. It has the lowest framework density (10.5 T-atoms per 1000 \AA^3) of all existing oxide zeolite frameworks.

EMM-23 ($[(N_2C_{19}H_{40})_3[Si_{64}O_{116}(OH)_{24}]]$) with the $*-EWT$ framework is the first stable three-dimensional extra-large pore (alumino)silicate zeolite.²⁰ The framework contains highly unusual tri-lobe shaped channels (Figure 2.24), which intersect with perpendicular 10-ring channels. The T-sites pointing towards the tri-lobe shaped channel are only partially occupied, and this leads to 21-ring channels when the T-sites are fully occupied (Figure 2.24a) or 24-ring channels when the T-sites are empty (Figure 2.24b). EMM-23 contains two- and three-connected T-atoms, with two or one terminal O atoms, respectively, protruding into the 21–24-ring channels.

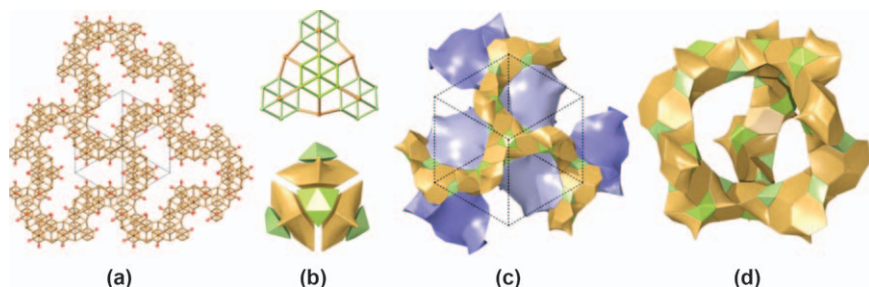


Figure 2.23 The $-ITV$ framework type. (a) A slice (15.3 Å thick) viewed down the $[111]$ direction. (b, c) The tile representation showing the framework (green and orange) and the channel system (blue). (d) The large cavity defined by three 30-rings. Reprinted by permission from Macmillan Publishers Ltd: *Nature*,³⁹ copyright (2009).

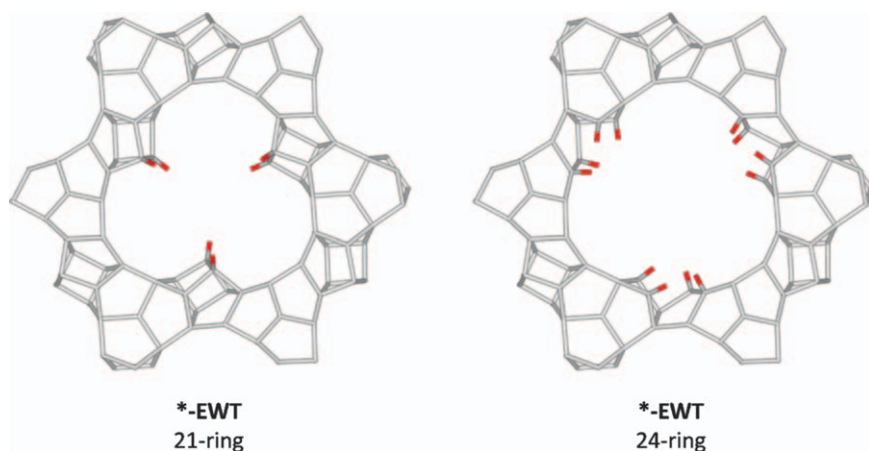


Figure 2.24 Structure of EMM-23 with the $*-EWT$ framework type viewed down the c -axis showing the channel in two extreme cases. The structure contains partially occupied T-sites pointing towards the channel, which leads to a 21-ring channel when the T-sites are fully occupied and a 24-ring channel when the T-sites are empty. Terminal O atoms are shown in red. Reprinted with permission from ref. 20. Copyright (2014) American Chemical Society.

2.5 Structure Determination

All the information in the examples above has been derived experimentally using crystallographic techniques. Crystal structure determination is routinely performed using single-crystal X-ray diffraction data, provided that crystals of large enough dimensions can be synthesized ($>10 \mu\text{m}$). However, synthetic zeolites are typically only available in polycrystalline form, and do not form

crystals large enough for such analyses. Nowadays, PXRD and electron diffraction are the most valuable experimental techniques for characterizing polycrystalline samples of zeolites. While PXRD data offers structural information on the entire bulk sample, electron diffraction provides information on individual crystallites in the sample. Of the 43 zeolite framework types approved since 2010, 34 were determined from the PXRD data alone or in combination with electron diffraction/high-resolution transmission electron microscopy (HRTEM) techniques. A brief overview of the use of PXRD and electron crystallography to characterize zeolites is given below.

2.5.1 Information in a Powder Diffraction Pattern

A powder diffraction pattern contains a lot of information about the zeolite sample being studied. Some of the most important features of a powder pattern are shown in Figure 2.25. While some of these readily offer qualitative information about the material, extracting quantitative information requires somewhat more expertise (see below).

In a powder diffraction pattern, the positions of the peaks (measured in 2θ) correspond to reflection positions. Note that a reflection does not necessarily give rise to a peak (the reflection may have an intensity of 0 depending on the crystal structure), but a peak always indicates the presence of a reflection. The reflections correspond to the lattice spacings (also referred to as d -spacings) and therefore are determined solely by the size and shape of the unit cell of the crystalline phase. The unit cell is the smallest representative unit in the crystal lattice that can be translated in three dimensions to describe the bulk atomic arrangement of the material. Each peak corresponds to at least one reflection, and each reflection is assigned to a Miller index (hkl value) in relation to the unit cell, in a procedure called *indexing*. This is straightforward for materials with small unit cells and high symmetry (e.g. those with cubic or hexagonal crystal systems), but is complicated by the

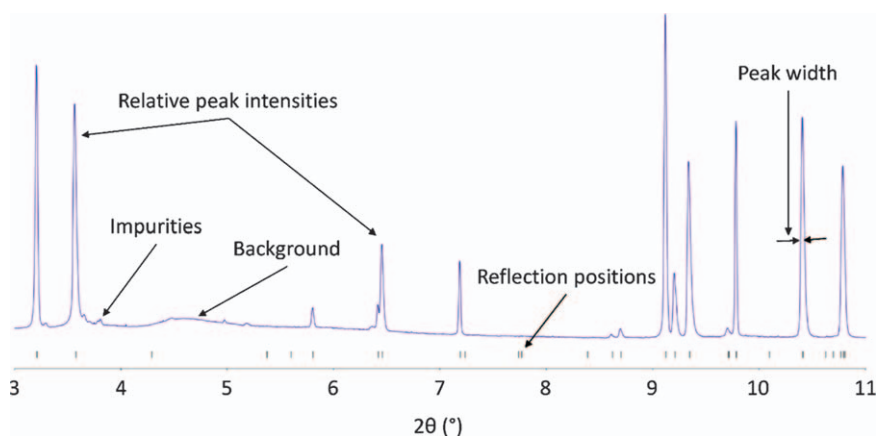


Figure 2.25 A powder diffraction pattern, with the features of interest highlighted.

fact that reflections that have similar d -spacings may overlap. Typically, overlapping reflections are undesirable, because they result in an ambiguity in the assignment of reflection intensities, which further complicates analysis. Note here that crystalline phases with larger unit cells or lower crystallographic symmetry will typically generate more reflections. If all reflections can be indexed with a single unit cell, this is a good indication that the phase is pure. If there are additional reflections present, unindexed by the unit cell, this may indicate the presence of an additional crystalline phase or that the unit cell is incorrect. Nowadays, a large number of reliable auto-indexing programs are available for determining the unit cell from a list of peak positions (2θ values or d -spacings).⁴⁰

If the positions of the reflections give information about the dimensions of the unit cell, then the relative reflection intensities describe the atomic decoration of the unit cell. In other words, the reflection intensities are related to the type and position of the atoms (*i.e.* electron density), and are the summation of all X-ray photons diffracted by the crystals. The intensities are therefore related to the average crystal structure of the sample being studied. It is important to note that even a small change in the crystal structure (*e.g.* after ion exchange) will involve all reflection intensities, although some may be more affected than others.

Peak widths can be used as a first indicator of crystal quality. Narrow peaks mean more well-defined unit cell parameters, and are preferred for structural analysis, because overlapping reflections can be resolved more easily. They are dependent on the intrinsic instrumental peak width, stress or strain, and crystallite size (or, more precisely, size of the coherent domain). The smaller the crystallites, the broader the peaks become, especially for those smaller than 1 μm . For small plate-like or needle-shaped crystals, reflection broadening may occur along one or two crystallographic directions, respectively, and is referred to as *anisotropic line broadening*.

The background in a powder pattern corresponds to everything that cannot be described by the zeolite crystal structure. A high background can indicate the presence of a large amount of amorphous material (*e.g.* unreacted gel), but air scatter, the tail of the direct beam, or the glass capillary can also contribute to the background. X-Ray fluorescence may also occur and add to the background, for example, if a Fe-containing material is measured using Cu $K\alpha$ radiation. This can be avoided by using a different wavelength.

2.5.2 Powder Diffraction for Phase Identification

The most widespread use of powder diffraction is for phase identification, because every zeolite framework structure produces a distinct diffraction pattern, which serves as a fingerprint for the material. Both the positions and the relative intensities of the reflections are characteristic for a particular phase, so identification can be performed by comparing the measured pattern to that of a known standard or previously prepared material. For this purpose, Treacy and Higgins put together the *Collection of Simulated*

XRD Powder Patterns for Zeolites,⁴¹ which contains calculated patterns of 226 zeolite materials representing 176 framework types. Although the book was published 10 years ago, it contains the most commonly encountered, and frequently synthesized, zeolites and is therefore a worthwhile resource to turn to. Nowadays, all this information is also available in the online Database of Zeolite structures. It is important to note that the presence of extra-framework species, and different heteroatoms, can affect the reflection intensities, unit cell, and symmetry, and this can hinder identification. 1

Furthermore, it is often possible to obtain the relative concentrations of several phases in a sample from a single diffraction pattern. It is relatively easy, and both time- and cost-efficient, to measure a diffraction pattern using a laboratory instrument. This is why powder diffraction is used extensively in industrial and academic laboratories for identification, characterization, and quality control. Provided the data quality is good enough, structure determination using PXRD data is also possible.⁴² 5 10 15

2.5.3 Structural Analysis using Powder Diffraction Data

It is often possible to follow structural changes in a material by evaluating differences in the relative peak intensities in the powder pattern. A difference in the powder diffraction pattern usually indicates that a modification of the crystal structure has occurred, and can be used as a simple method to see whether a post-synthesis treatment has had the desired effect. For example, non-framework species have a noticeable effect on the relative intensities in the low-angle region. A calcined material typically has higher relative peak intensities in this region than does an as-synthesized material. The high-angle region is usually less sensitive to the presence of electron density in the zeolite channels, and more affected by small deviations in the atomic positions from the ideal framework positions, atomic displacement (thermal vibrations of the atoms), defects, bond lengths, and presence of heteroatoms. 20 25 30

To extract more detail from the powder pattern, a full Rietveld (whole-profile) structure refinement should be performed.^{43,44} The Rietveld method is used to complete, refine, and validate a structural model, by calculating the diffraction pattern corresponding to the model and comparing it to the experimental pattern. By minimizing the difference between the observed and calculated powder pattern *via* a least-squares minimization routine, the structural parameters of the model can be improved. In this way, depending on the quality of the powder pattern, accurate quantitative information can be extracted. 35 40

It is generally accepted that the locations of inorganic cations of an as-synthesized or ion-exchanged zeolite can be found in difference electron density maps during the course of a Rietveld refinement. Locating the organic cation is more difficult, because the organic compounds consist of light scatterers and typically have low point symmetry, while the zeolite hosts consist of heavier scatterers and tend to adopt higher symmetries. These features result in a lack of contrast that makes it difficult to 'see' the organic guest species, but their 45

positions can generally be located through a careful difference electron density calculation and interpretation combined with Rietveld refinement.⁴⁵ 1

The location of heteroatoms (*e.g.* Ge in germanosilicates or B in borosilicates) can sometimes be determined during the refinement process. Provided the population of the heteroatom is high enough, a difference electron density map will readily reveal its position. The notable exception here is Al in aluminosilicates, which is notoriously difficult to find, because the contrast in X-ray diffraction comes from the difference in electron density, and Si and Al have very similar scattering characteristics. However, the bond distances of Si–O (~ 1.61 Å) and Al–O (~ 1.74 Å) are different, and this can sometimes be used to indirectly distinguish the two. 5 10

2.5.4 Electron Diffraction

Electron diffraction (ED) is complementary to PXRD, and can also be used for phase identification and structural analysis. Each crystallite in a powder sample behaves like a single crystal in ED, and there is no peak overlap in ED. Thus ED has a unique advantage for studying multiphasic samples. Normally, an ED pattern is obtained by selecting one crystallite, aligning it along a crystallographic axis (zone axis), and recording the pattern of the selected crystallite. An ED pattern is a 2D section of the 3D reciprocal lattice that can be used as a fingerprint for phase identification. The two shortest reciprocal lattice vectors (in Å^{-1}) and the angle between them can be determined from the ED pattern. They are compared with those calculated for a given zeolite. If these three values fit, it is likely that the ED pattern is from that zeolite. However, in some cases, more than one zeolite might fit an ED pattern, especially if the ED pattern is taken along a zone axis with high indices or if the zeolite structures have some identical projections. To resolve the ambiguity, more than one ED pattern should be taken from the same crystal, and all ED patterns and the tilt angles between them should be used to search for the best fit.⁴⁶ 15 20 25 30

Recently, new 3D ED methods were developed, in particular automated diffraction tomography (ADT)⁴⁷ and rotation electron diffraction (RED),⁴⁸ for collecting a series of ED patterns from an arbitrarily oriented crystal. Almost complete 3D ED data can be collected. Phase identification is much easier using 3D ED data. The 3D peak positions and peak intensities can be extracted from the ADT/RED data and combined into a 3D reciprocal lattice. The unit cell parameters can be determined directly from this reconstructed reciprocal lattice.^{47,48} Possible space groups can be deduced from the systematically absent reflections. The unit cell and space group are used to identify the zeolite. 35 40

In addition to unit cell and space group determination, the 3D ED data can also be used to determine the structure of a new zeolite. The procedure is similar to that used to determine a structure from single-crystal X-ray diffraction. The advantage is that the same software can be used with the 3D ED data. A large number of zeolite structures have been solved using 3D ED data,⁴⁹ one example (ITQ-51, IFO) is shown in Figure 2.26.⁵⁰ 45

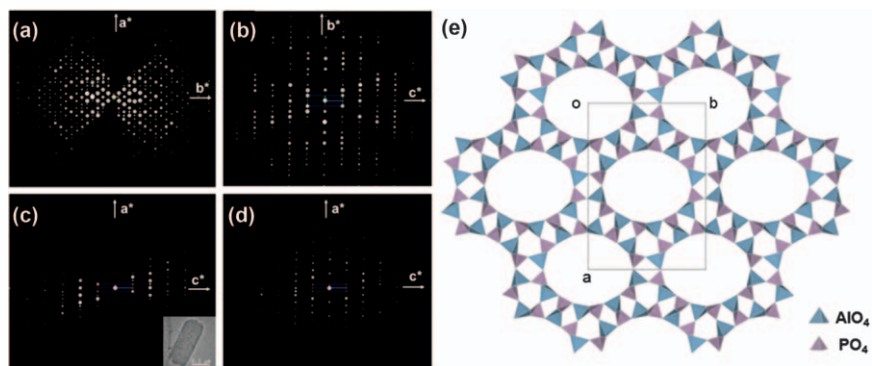


Figure 2.26 (a–d) 2D slices of the reciprocal lattice of ITQ-51 (IFO),⁵⁰ copyright (2013) National Academy of Sciences, reconstructed from the 3D RED data. (a–c) 2D slices from the crystal shown in the inset of (c). (d) 2D ($h0l$) slice from a different crystal, showing that the two datasets cover different parts of reciprocal space. (e) Structural model for ITQ-51 viewed along the c -axis.

AQ:4

For phase identification, it is important to calibrate the camera length and ensure that the crystal is at the eucentric height so that the d -values are determined accurately. For structure determination, it is important to collect the ED data from very thin crystals (<100 nm) in order to minimize dynamical effects and thereby obtain more kinematical ED intensities.

2.5.5 Structural Analysis using HRTEM Images

High-resolution transmission electron microscopy (HRTEM) images can also be used for phase identification and structure determination, but this technique is more demanding.⁴⁹ Both the crystallographic amplitude and phase information can be extracted from HRTEM images and used for structure determination. HRTEM has unique advantages for studying disordered zeolite materials, because the local atomic arrangement can be observed directly. One such example is the determination of the structure of ITQ-39 (*-ITN) using HRTEM images taken along two perpendicular crystallographic axes.¹⁹ Twinning and stacking disorders can be visualized directly from the HRTEM images (Figure 2.27). The structure factor amplitudes and phases were obtained from very small regions free of defects and used to reconstruct the 3D electrostatic map, from which the structural model could be obtained (Figure 2.27).

Electron crystallography is powerful for structure identification and structure solution from individual nano- or micron-sized particles, and PXRD provides information from all phases present in the sample (the bulk material). While electron crystallography suffers from dynamical scattering, PXRD data are kinematical. Therefore, electron crystallography and PXRD are highly complementary and their combination is a powerful one for studying multiphasic samples and complicated crystal structures.

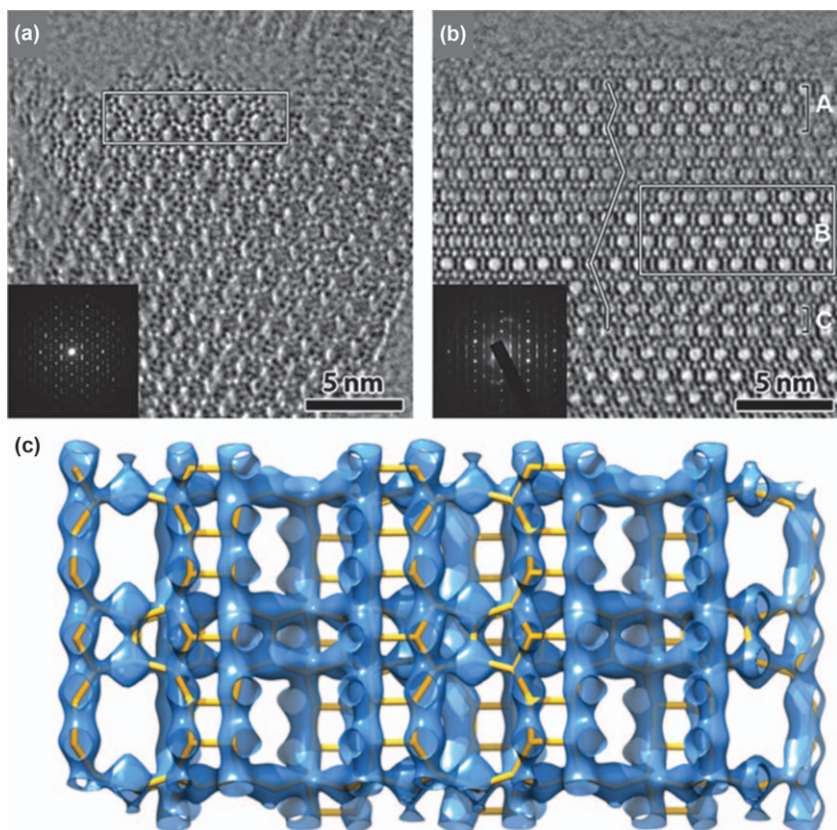


Figure 2.27 HRTEM images of ITQ-39 (*-ITN) taken along (a) [010] and (b) [100]. The domains used for structure factor determination are outlined by rectangles. (c) The 3D electrostatic potential map reconstructed from the structure factor amplitudes and phases extracted from the marked domains with the refined structural model superimposed.

Reprinted by permission from Macmillan Publishers Ltd: Nature Chemistry,¹⁹ copyright (2012).

2.6 Conclusions

Despite the fact that the basic building unit of a zeolite is a simple TO_4 tetrahedron, these can be arranged in an infinitely large number of ways. Researchers are applying increasingly sophisticated synthesis techniques to produce materials with increasingly complex framework structures. So far, the online Database of Zeolite Structures contains only unique 232 framework structures corresponding to materials whose structures have been determined to the satisfaction of the Structure Commission of the International Zeolite Association. Of those, 13 important, relevant, or otherwise interesting framework structures have been selected, not only to highlight the great structural variety present in zeolites but also the features that bind

them. Different ways of characterizing features common to different framework types, such as building units, ring sizes and channel systems, vertex symbols, and coordination sequences, have been described. 1

In addition to the framework architecture, other structural features such as chemical composition and the positions of heteroatoms, the location of extra-framework cations and guest species absorbed in the pores, and stacking faults or defects have been discussed. To fully understand a material's properties, all these aspects should be considered. Several examples have been highlighted throughout this chapter. 5

Widely accessible methods, such as PXRD, 3D ED, and HRTEM, can be used for phase identification and structural analysis of zeolite materials. These techniques are highly complementary and the combination needed depends upon the information required. 10

Acknowledgements 15

The authors thank Lynne B. McCusker and Christian Baerlocher for useful insights into some more obscure details of zeolite structural science, and comments on the manuscript. S. S. thanks the Swiss National Science Foundation for financial support (project number: 165282). 20

References

1. W. M. Meier and D. H. Olson, *Atlas of Zeolite Structure Types*, Polycrystal Book Service, Pittsburgh, 1978. 25
2. P. Guo, W. Wan, L. McCusker, C. Baerlocher and X. Zou, *Z. Kristallogr. – Cryst. Mater.*, 2015, **230**, 301–309.
3. T. Willhammar and X. Zou, *Z. Kristallogr. – Cryst. Mater.*, 2012, **228**, 11–27.
4. N. A. Anurova, V. A. Blatov, G. D. Ilyushin and D. M. Proserpio, *J. Phys. Chem. C*, 2010, **114**, 10160–10170. 30
5. V. A. Blatov, O. Delgado-Friedrichs, M. O’Keeffe and D. M. Proserpio, *Acta Crystallogr. A*, 2007, **63**, 418–425.
6. V. A. Blatov, *Struct. Chem.*, 2012, **23**, 955–963.
7. P. Guo, J. Shin, A. G. Greenaway, J. G. Min, J. Su, H. J. Choi, L. Liu, P. A. Cox, S. B. Hong, P. A. Wright and X. Zou, *Nature*, 2015, **524**, 74–78. 35
8. W. M. Meier and H. J. Moeck, *J. Solid State Chem.*, 1979, **27**, 349–355.
9. M. O’Keeffe and S. T. Hyde, *Zeolites*, 1997, **19**, 370–374.
10. W. Loevenstein, *Am. Mineral.*, 1954, **39**, 92–96.
11. W. J. Mortier, *Compilation of Extra Framework Sites in Zeolites*, Butterworth Scientific Limited, Guildford, 1982. 40
12. C. Baerlocher and W. M. Meier, *Helv. Chim. Acta*, 1969, **52**, 1853–1860.
13. C. Baerlocher and W. M. Meier, *Helv. Chim. Acta*, 1970, **53**, 1285–1293.
14. C. Baerlocher and W. M. Meier, *Z. Kristallogr.*, 1972, **135**, 339–354.
15. G. D. Price, J. J. Pluth, J. V. Smith, T. Araki and J. M. Bennett, *Nature*, 1981, **292**, 818–819. 45

16. G. D. Price, J. J. Pluth, J. V. Smith, J. M. Bennett and R. L. Patton, *J. Am. Chem. Soc.*, 1982, **104**, 5971–5977. 1
17. R. Catlow, R. Bell, F. Cora and B. Slater, in *Introduction to Zeolite Science and Practice*, ed. J. Cejka, H. van Bekkum, A. Corma and F. Schüth, 2007, vol. 168, pp. 659–700. 5
18. Y. Yu and R. Xu, *Acc. Chem. Res.*, 2010, **43**, 1195–1204.
19. T. Willhammar, J. Sun, W. Wan, P. Oleynikov, D. Zhang, X. Zou, M. Moliner, J. Gonzalez, C. Martínez, F. Rey and A. Corma, *Nat. Chem.*, 2012, **4**, 188–194.
20. T. Willhammar, A. W. Burton, Y. Yun, J. Sun, M. Afeworki, K. G. Strohmaier, H. Vroman and X. Zou, *J. Am. Chem. Soc.*, 2014, **136**, 13570–13573. 10
21. C. Baerlocher, T. Weber, L. B. McCusker, L. Palatinus and S. I. Zones, *Science*, 2011, **333**, 1134–1137.
22. S. Smeets, D. Xie, C. Baerlocher, L. B. McCusker, W. Wan, X. Zou and S. I. Zones, *Angew. Chem.*, 2014, **126**, 10566–10570. 15
23. M. M. J. Treacy, J. M. Newsam and M. W. Deem, *Proc. R. Soc. London, Ser. A*, 1991, **433**, 499–520.
24. T. Proffen and R. B. Neder, *J. Appl. Crystallogr.*, 1997, **30**, 171–175.
25. M. Casas-Cabanas, J. Rodríguez-Carvajal and M. R. Palacín, *Z. Kristallogr. Suppl.*, 2006, **23**, 243–248. 20
26. A. A. Coelho, J. S. O. Evans and J. W. Lewis, *J. Appl. Crystallogr.*, 2016, **49**, 1740–1749.
27. M. M. J. Treacy, D. E. W. Vaughan, K. G. Strohmaier and J. M. Newsam, *Proc. R. Soc. London, Ser. A*, 1996, **452**, 813–840. 25
28. G. Perego, M. Cesari and G. Allegra, *J. Appl. Crystallogr.*, 1984, **17**, 403–410.
29. T. Ohsuna, O. Terasaki, Y. Nakagawa, S. I. Zones and K. Hiraga, *J. Phys. Chem. B*, 1997, **101**, 9881–9885.
30. W. J. Roth and D. L. Dorset, *Microporous Mesoporous Mater.*, 2011, **142**, 32–36. 30
31. T. Conradsson, M. Dadachov and X. Zou, *Microporous Mesoporous Mater.*, 2000, **41**, 183–191.
32. T. Blasco, A. Corma, M. J. Díaz-Cabañas, F. Rey, J. A. Vidal-Moya and C. M. Zicovich-Wilson, *J. Phys. Chem. B*, 2002, **106**, 2634–2642. 35
33. G. Sastre, A. Pulido, R. Castañeda and A. Corma, *J. Phys. Chem. B*, 2004, **108**, 8830–8835.
34. P. Kamakoti and T. A. Barckholtz, *J. Phys. Chem. C*, 2007, **111**, 3575–3583.
35. W. J. Roth, P. Nachtigall, R. E. Morris, P. S. Wheatley, V. R. Seymour, S. E. Ashbrook, P. Chlubná, L. Grajciar, M. Položij, A. Zukal, O. Shvets and J. Čejka, *Nat. Chem.*, 2013, **5**, 628–633. 40
36. E. Verheyen, L. Joos, K. Van Havenbergh, E. Breynaert, N. Kasian, E. Gobechiya, K. Houthoofd, C. Martineau, M. Hinterstein, F. Taulelle, V. Van Speybroeck, M. Waroquier, S. Bals, G. Van Tendeloo, C. E. A. Kirschhock and J. A. Martens, *Nat. Mater.*, 2012, **11**, 1059–1064. 45

37. P. Chlubná-Eliášová, Y. Tian, A. B. Pinar, M. Kubru, J. Cejka and R. E. Morris, *Angew. Chem.*, 2014, **126**, 7168–7172. 1
38. M. Shamzhy, M. Opanasenko, Y. Tian, K. Konysheva, O. Shvets, R. E. Morris and J. Cejka, *Chem. Mater.*, 2014, **26**, 5789–5798.
39. J. Sun, C. Bonneau, A. Cantin, A. Corma, M. J. Díaz-Cabañas, M. Moliner, D. Zhang, M. Li and X. Zou, *Nature*, 2009, **458**, 1154–1157. 5
40. J. Bergmann, A. Le Bail, R. Shirley and V. Zlokazov, *Z. Kristallogr. – Cryst. Mater.*, 2004, **219**, 783–790.
41. M. M. J. Treacy and J. B. Higgins, *Collection of Simulated XRD Powder Patterns for Zeolites Fifth (5th) Revised Edition*, Elsevier, 2007. 10
42. W. I. F. David and K. Shankland, *Acta Crystallogr. A*, 2008, **64**, 52–64.
43. R. A. Young, *The Rietveld Method*, Oxford University Press, 1993.
44. L. B. McCusker, R. B. Von Dreele, D. E. Cox, D. Louër and P. Scardi, *J. Appl. Crystallogr.*, 1999, **32**, 36–50.
45. S. Smeets, L. B. McCusker, C. Baerlocher, S. Elomari, D. Xie and S. I. Zones, *J. Am. Chem. Soc.*, 2016, **138**, 7099–7106. 15
46. X. Zou, S. Hovmöller and P. Oleynikov, *Electron Crystallography*, Oxford Science Publications, 2011.
47. U. Kolb, T. Gorelik, C. Kübel, M. T. Otten and D. Hubert, *Ultramicroscopy*, 2007, **107**, 507–513. 20
48. W. Wan, J. Sun, J. Su, S. Hovmöller and X. Zou, *J. Appl. Crystallogr.*, 2013, **46**, 1863–1873.
49. T. Willhammar, Y. Yun and X. Zou, *Adv. Funct. Mater.*, 2014, **24**, 182–199.
50. R. Martínez-Franco, M. Moliner, Y. Yun, J. Sun, W. Wan, X. Zou and A. Corma, *Proc. Natl. Acad. Sci. U. S. A.*, 2013, **110**, 3749–3754. 25

30

35

40

45